agronomy

MDPI

Article

Phenylalanine Ammonia-Lyase (PAL) Genes Family in Wheat (*Triticum aestivum* L.): Genome-Wide Characterization and Expression Profiling

Fatima Rasool [1,2], Muhammad Uzair [2], Muhammad Kashif Naeem [2], Nazia Rehman [2], Amber Afroz [3], Hussain Shah [4] and Muhammad Ramzan Khan [1,2,*]

1 Genome Editing & Sequencing Lab, National Centre for Bioinformatics, Quaid-i-Azam University, Islamabad 45320, Pakistan; fatimarasool014@yahoo.com
2 National Institute for Genomics and Advanced Biotechnology, National Agricultural Research Centre, Park Road, Islamabad 45500, Pakistan; uzairbreeder@gmail.com (M.U.); kashifuaar@gmail.com (M.K.N.); naziarehman96@yahoo.com (N.R.)
3 Department of Biochemistry and Biotechnology, University of Gujrat, Gujrat 50700, Pakistan; dramber.afroz@uog.edu.pk
4 Pakistan Agriculture Research Council, Park Road, Islamabad 44000, Pakistan; hussainshah05@yahoo.com
* Correspondence: mrkhan@parc.gov.pk; Tel.: +92-51-8443705

Abstract: Phenylalanine ammonia-lyase (PAL) is the first enzyme in the phenylpropanoid pathway and plays a vital role in adoption, growth, and development in plants but in wheat its characterization is still not very clear. Here, we report a genome-wide identification of *TaPAL* genes and analysis of their transcriptional expression, duplication, and phylogeny in wheat. A total of 37 *TaPAL* genes that cluster into three subfamilies have been identified based on phylogenetic analysis. These *TaPAL* genes are distributed on 1A, 1B, 1D, 2A, 2B, 2D, 4A, 5B, 6A, 6B, and 6D chromosomes. Gene structure, conserved domain analysis, and investigation of *cis*-regulatory elements were systematically carried out. Chromosomal rearrangements and gene loss were observed by evolutionary analysis of the orthologs among *Triticum urartu*, *Aegilops tauschii*, and *Triticum aestivum* during the origin of bread wheat. Gene ontology analysis revealed that *PAL* genes play a role in plant growth. We also identified 27 putative miRNAs targeting 37 *TaPAL* genes. The high expression level of *PAL* genes was detected in roots of drought-tolerant genotypes compared to drought-sensitive genotypes. However, very low expressions of *TaPAL10*, *TaPAL30*, *TaPAL32*, *TaPAL3*, and *TaPAL28* were recorded in all wheat genotypes. Arogenate dehydratase interacts with TaPAL29 and has higher expression in roots. The analysis of all identified genes in RNA-seq data showed that they are expressed in roots and shoots under normal and abiotic stress. Our study offers valuable data on the functioning of *PAL* genes in wheat.

Keywords: phenylalanine ammonia-lyase (PAL); phylogenetic analysis; expression profiling; gene structure; drought stress

Citation: Rasool, F.; Uzair, M.; Naeem, M.K.; Rehman, N.; Afroz, A.; Shah, H.; Khan, M.R. Phenylalanine Ammonia-Lyase (PAL) Genes Family in Wheat (*Triticum aestivum* L.): Genome-Wide Characterization and Expression Profiling. *Agronomy* **2021**, *11*, 2511. https://doi.org/10.3390/agronomy11122511

Academic Editors: Channapatna S. Prakash, Ali Raza, Xiling Zou and Daojie Wang

Received: 18 October 2021
Accepted: 20 November 2021
Published: 10 December 2021

1. Introduction

Phenylalanine ammonia-lyase (PAL) produces precursors of various secondary metabolites, including lignin, phytoalexin, and phenolic compounds. This gene family is also associated with the production of the first enzyme of the phenylpropanoid pathway [1–3]. *PAL* genes have a molecular mass in the range of 270–330 kilodalton (kDa) and are present in higher plants, yeast, some bacteria, and fungi. However, these genes are not found in animals because they have another histidine ammonia lyase (HAL) [4]. The PAL family encodes a variety of protective compounds such as components of the cell wall, flavonoids, phytoalexins, and furanocoumarin [5,6]. The conversion of L-phenylalanine to cinnamic acid, linking primary metabolism with secondary metabolism catalyzed by the PAL enzymes, also plays an essential role in phenylpropanol biosynthesis, a speed-limiting step in

phenylpropanol metabolism [1].This metabolic pathway is involved in the production of various natural products (phytoalexin, hydroxycinnamic acids, flavonoids, etc.), and is also reported as a role player in phenolic glycoside and benzene compound synthesis, which are part of several enzyme-regulated reactions [1,2,7–10]. Thus, phenylpropanoids play a critical role for the growth, development, and survival of vascular plants [1]. *PAL* activity is induced dramatically in reply to various stimuli such as tissue wounding, pathogenic attack, light, low temperature, and hormonal triggers [5,11].

The first plant PAL was found in *Petroselinum crispum* in crystal forms [12]. The *PAL* encoding genes are typically discovered as small gene families comprising one to five members [13,14]. During the evolution of higher plants, PAL diversified into different functions. Both HAL and PAL have different primary protein sequences, but they perform similar functions *in vivo*. It was thought that PAL is formed from HAL when the fungi and plants separated from other kingdoms [15,16]. There are two (the first is horizontal gene transfer (HGT) and the second is gene duplication) methods of evolution are reported. Studies showed that gene duplication is the major method of evolution and gymnosperms are thought to be the ancestors of angiosperms [16,17]. For instance, four *PAL* gene family members in *Arabidopsis thaliana* [18,19], five in *Populus trichocarpa* [20], three in *Scutellaria baicalensis* [21], and three in *Coffeac anephora* [22] have been recognized and functionally described. Nevertheless, some studies have indicated more than five *PAL* genes in certain plants. Moreover, five separate *PAL* genes were recognized in *Pinus taeda* [23]. Furthermore, as many as thirteen *PAL* genes were discovered in *Cucumis sativus* [24], twelve in *Citrullus lanatus* [24], thirteen in *Cucumis melo,* and sixteens in *Vitis vinifera* [25].

Wheat (*Triticum aestivum*) is an important source of starch, protein, and minerals in the diet for more than 35% of the world's inhabitants. It is grown on a variety of soil and in a range of environmental conditions [26]. To prevent environmental stresses, the wheat plant has evolved multiple plant protection systems [27]. Previous studies showed the involvement of the *PAL* gene family in coping with the environmental stresses by activating the transcriptional processes. The *PAL* gene family is responsible for the adaptation and resistance of plants to unfavorable biotic and abiotic environmental conditions. It also controls the expression and inhibition of genes to amend different biochemical pathways. Our research explored, a theoretical way. the functional characterization, and differential expression analysis of the *PAL* gene family engaged in the root development of six different wheat genotypes. This study carries immense importance in understanding the stress tolerance mechanisms in wheat and the role of the *PAL* gene family in the same.

2. Materials and Methods

2.1. Retrieval of Protein Sequences Containing the PAL Gene Family in Triticum aestivum

Two methods were applied to retrieve the phenylalanine ammonia-lyase (PAL) domain-containing sequences in wheat. The first method searched the *PAL* gene family members in the *Triticum aestivum* by inputting the keywords "Phenyl ammonium lyase (PAL)" in the Ensembl plants database (http://plants.ensembl.org/Triticum_aestivum/ (accessed on 16 March 2021) [28], while in the second method, the search for wheat *PAL* genes was conducted using *Arabidopsis thaliana PAL* genes (*At3g53260*, *At2g37040*, *At3g10340*, and *At5g04230*) as reference/query to BLASTP [29] against wheat protein database International Wheat Genome Sequencing Consortium (IWGSC) (V2.1), and *Triticum aestivum* chromosome 3B RELEASE 1.0 (http://wheat-urgi.versailles.inra.fr/, accessed on 16 April 2021). Based on more than 75% sequence identity and E-value $\leq$ 1e-10, the wheat *PAL* gene family was identified. Unique non-redundant wheat PAL gene family members were identified by performing multiple sequence alignments using the ClustalW tool [30], and redundant gene sequences were removed. Further, the Pfam [31] and SMART (http://smart.embl-heidelberg.de/, accessed on 18 May 2021) databases [32] were used for the identification and confirmation of PAL-conserved domains.

2.2. Gene Structure and Conserved Domain Analysis of TaPAL Genes

The online Gene Structure Display Server GSDS 2.0 (http://gsds.gao-lab.org/, accessed on 20 May 2021) [33] was used to examine the gene structure by comparing the open reading frame (ORF) sequence with the corresponding genomic sequences. The conserved motifs of TaPAL protein analysis were determined by MEME Suit (Multiple EM for Motif Elicitation) Version 4.12.0 (http://meme-suite.org/tools/meme, accessed on 25 May 2021) [34] using the following parameters: the number of motifs to be found was ten, and the motif width was kept between 10 and 200; site distribution was set at zero or one occurrence per sequence (thus each sequence was allowed to contain at most one occurrence of each motif). The chromosomal location was drawn on respective chromosomes. The molecular weight (g/mol), isoelectric point, protein charge, and the subcellular location were retrieved from UniProt (https://www.uniprot.org, accessed on 28 May 2021) [35]. The conserved domains of TaPAL proteins were examined using the Unipro UGENE software package [36], which joined the sequences into alignment by the ClustalW algorithm and displayed conservation in the form of color patterns differentiating each amino acid based on physiochemical properties. Protein domain analysis was also performed by using TaPAL1 protein sequence and SMART database containing Pfam domain search option (https://pfam.xfam.org/, accessed on 18 November 2021), and confirmed through the InterPro (https://www.ebi.ac.uk/interpro/, accessed on 18 November 2021) database [37].

2.3. Phylogenetic Identification

To retrieve the protein sequence containing the PAL domain, 37 protein sequences of wheat were used as queries to BLASTP against the *Triticum urartu*, *Solanum tuberosum,* and *Hordeum vulgare*. The protein sequences with more than 70% sequence identity were downloaded from NCBI (https://www.ncbi.nlm.nih.gov/, accessed on 16 June 2021). The *PAL* genes of *Arabidopsis thaliana, Zea mays,* and *Oryza sativa* were retrieved from Ensembl (http://plants.ensembl.org, accessed on 18 June 2021). Molecular Evolutionary Genetics Analysis (MEGA version X) [38] was used to infer the evolutionary history of TaPAL by the maximum-likelihood (ML) method and 1000 bootstrap replicates were used. While the gene duplication was calculated by using MCScanX in Tbtools [39].

2.4. Synteny Analysis

The visualization sequence identity and synteny analysis of the *PAL* family genes were performed using Tbtools [40]. These analyses were used to study the sequence similarity patterns [41].

2.5. miRNA Prediction in Wheat PAL Family Genes

miRNA prediction was carried out as previously described [42]. In detail, all the genome sequences of *TaPAL* genes were submitted against the available reference of miRNA sequences using the psRNATarget Server (https://www.zhaolab.org/psRNATarget/, accessed on 14 September 2021) with default setting [43]. While the visualization of interaction was carried out with the help of Cytoscape software (https://cytoscape.org/, accessed on 14 September 2021) by following the default setting [44].

2.6. Promoter and Gene Ontology (GO) Enrichment Analysis

The upstream 1 kb nucleotide sequence from the start codon was retrieved for promoter analysis of all the 37 *TaPAL* genes using the Ensembl Plants database (http://plants.ensembl.org/Triticum_aestivum/, accessed on 19 June 2021). Subsequently, these were also subjected to identification of the already-defined motif by using the PLACE *cis*-regulatory element database [2,45]. These databases also helped to obtain five *cis*-regulatory elements (CACTFTPPCA1, CATTBOX1, ARR1AT, CGCGBOXAT, and WBOXNTERF) and their location. GO analysis of TaPAL protein sequences was conducted by using online

tool gProfiler (https://biit.cs.ut.ee/gprofiler/gost, accessed on 20 June 2021) with default parameters [46].

2.7. Protein–Protein Interaction

Protein–protein interactions of wheat were analyzed by using the STRING online server (http://string.embl.de, accessed on 14 September 2021) with the default setting [47].

2.8. Analysis of RNA-Seq Base expression profiling

Six different wheat varieties (Table 1) were used to analyze *PAL* RNA-seq base expression profiling of the *TaPAL* genes. All the wheat varieties were grown under normal conditions at the National Agricultural Research Centre (NARC), Islamabad, Pakistan. The root samples (each data point pooled from eight plants) were collected as previously described [48,49] from 35-day-old seedlings of all six wheat varieties and were frozen in liquid nitrogen prior to storage at −80 °C until use. Total RNA of the above-prepared samples was isolated using the Gene JET™ Plant RNA Purification Mini Kit (Catalog # K0801). Illumina HiSeq2500 platform was used for paired-end (PE) sequencing of wheat RNA samples. The quality of raw data was checked with the help of FastQC (http://www.bioinformatics.bbsrc.ac.uk/projects/fastqc/, accessed on 25 June 2021). Trimming of reads (quality scores < 20) was done with the help of the Trimmomatic tool [50]. The HISAT2 (version 2.0.5) (http://ccb.jhu.edu/software/hisat2/faq.shtml, accessed on 28 June 2021) tool with default settings [51] was used for constructing a transcriptome map based on the genome reference of wheat (ftp://ftp.ensemblgenomes.org/pub/release-25/plants/fasta/triticum_aestivum/dna/, accessed on 4 July 2021). The transcripts were assembled with String Tie software [52], while the NOIseq package was used to find the expression level of genes and transcripts and to draw the graph of the genes. The NOIseq package [53] was used to calculate the FPKM (fragments per kilobase per million) mapped. The genes with FPKM values greater than one were retained for subsequent analyses.

Table 1. Wheat genotypes used for RNA-seq analysis.

Genotypes	Characteristics
Batis	Winter wheat (drought-susceptible) from Germany (INRES)
Blue Silver	Spring wheat (drought-susceptible) was released in Pakistan in 1971 by the NARC
Chakwal-50	Released in 2008 as drought-tolerant, high-yielding, and disease-resistant wheat grown in rain-fed areas of Pakistan by BARI
Local White	Drought-tolerant land race, grown in dryer areas of Pakistan (NARC)
Syn-22	Synthetic wheat (drought-tolerant) from The Netherlands (INRES)
UZ-11-CWA-8	Drought-tolerant line collected from Uzbekistan (INRES)

The expression levels were also analyzed at different stages in root and shoot tissues in response to abiotic stress (drought, heat, combination of both, Supplementary Sheet S1). The RNA-seq data was retrieved in transcripts per million (TPM) from the expVIP [54] wheat expression browser (http://www.wheat-expression.com/, accessed on 6 August 2021). To check the expression patterns of a given *PAL* gene subjected to abiotic stress, the ratio of the expression under treatment to the control was calculated (ratio ≥ 1 = altered under stress; ratio ≤ 1 = un-altered under stress). Finally, a heatmap was constructed by R package pheatmap (version 1.7) [55].

3. Results

3.1. Common Wheat PAL Gene Characterization and Identification

Systematic approaches were used to identify and characterize *TaPAL* genes from the *T. aestivum* genome using various genomic resources and tools. Finally, 37 full-length coding *PAL* genes were identified. The results evidenced that the 37 sequences containing *PAL*-HAL domains belonged to the *PAL* gene family (Supplementary File S1). The detailed information on these identified genes, including gene ID, chromosomal location, start and

ending genomic position, protein length, and other related information, are summarized in Table 2. The stability of protein can be checked through the number of amino acids. The peptide length of deduced TaPAL proteins ranged from 498 (*TaPAL37*) to 714 (*TaPAL7*) amino acids with corresponding molecular weights ranging from 52.78 to 77.34 kDa with an average weight 74.97 kDa. Their predicted isoelectric (IP) points varied from 5.76 (*TaPAL35*) to 7.57 (*TaPAL31*), indicating that different TaPAL proteins function in different microenvironments. This IP value was used to measure the net charge on the proteins. The proteins with IP < 7 were considered as acidic and IP > 7 as basic. Thirty-five of the 37 *TaPAL* genes were acidic in nature. In addition, analysis of the subcellular localization of the *T. aestivum* indicated that all 37 PAL transcripts are localized in the cytoplasm (Table 2).

3.2. Localization of TaPAL Genes on the Chromosomes

The predicted *TaPAL* genes were localized on *Triticum aestivum* chromosomes. For this purpose, 37 *TaPAL* genes were mapped to chromosomes of common wheat based on physical positions, as shown in Figure 1. Our results showed that the distribution pattern of the *TaPAL* genes was different on each chromosome. The maximum number (six) of *PAL* genes were present on chromosome 1B and 2B followed by chromosome 2A (five genes), chromosome 2D (four genes), and chromosomes 1A, 1D, 6B, and 6D (three genes each), while chromosome 5B had two genes. The remaining chromosomes (4A and 6A) each contained a single gene. The shortest chromosome was 6D with three genes, while the largest chromosome was 2B containing six genes. Some genes were far away from each other, and some genes were in cluster form, which indicates that these may contains a single QTL. Thus, the chromosomal localization studies revealed an uneven distribution of the 37 candidate genes on all the chromosomes of *T. aestivum* (Figure 1). In nature there are two types of duplication involved in evolution. The first is first tandem duplication (among two or more genes on the same chromosome) and the second is segmental duplication (among different chromosomes and the same clades). *TaPAL25/TaPAL7*, *TaPAL33/TaPAL29*, *TaPAL37/TaPAL18*, *TaPAL25/TaPAL14*, *TaPAL33/TaPAL11*, *TaPAL37/TaPAL27*, *TaPAL18/TaPAL27*, *TaPAL1/TaPAL14*, *TaPAL29/TaPAL11*, *TaPAL34/TaPAL22*, *TaPAL12/TaPAL23*, *TaPAL36/TaPAL35*, *TaPAL34/TaPAL16*, *TaPAL22/TaPAL16*, *TaPAL24/TaPAL3*, *TaPAL24/TaPAL19*, *TaPAL28/TaPAL26*, *TaPAL32/TaPAL30*, and *TaPAL3/TaPAL19* are segmentally duplicated in wheat.

3.3. Identification of Conserved Protein Domains and Motifs in TaPAL Proteins

The MEME server was used to analyze the conserved domains (motifs) within the TaPAL gene family. The MEME program resulted in the identification of 10 conserved motifs of the 37 TaPAL members (Figure 2). The length of the predicted motifs ranged from 40 to 49 amino acids. Motif 9 and motif 10 were primarily present in all genes except the *TaPAL13*, *TaPAL37*, and *TaPAL31* genes. Figure 2B shows that motifs 8, 9, and 10 were not present on the *TaPAL37* gene. Furthermore, motifs 1–7 were conserved in all groups of the phylogenetic tree. The SMART database's result indicated that all *TaPAL* genes contain a well-conserved aromatic lyase domain (PF00221) [56]. This domain (e-value 2.4e-153) starts from 56 aa and ends at 536 aa (Figure 2D and Supplementary File S2).

Table 2. Detailed information of *TaPAL* genes in wheat.

Sr.#	Gene ID	Name	Subcellular Location	AA	MW (g/mol)	IP	Charge	Chrom	Gene Position Start–End (bp)	St
1	TraesCS1B02G048400	*TaPAL1*	Cytoplasm	707	76,625.34	6.2111	−3.5	1B	28,442,914–28,445,758	R
2	TraesCS1B02G048300	*TaPAL2*	Cytoplasm	713	77,090.98	6.0532	−5.0	1B	28,373,087–28,375,944	R
3	TraesCS6B02G258600	*TaPAL3*	Cytoplasm	712	76,561.87	6.2119	−3.0	6B	465,682,950–465,685,480	R
4	TraesCS2A02G381000	*TaPAL4*	Cytoplasm	713	77,163.92	5.9516	−6.0	2A	624,446,955–624,449,699	F
5	TraesCS2D02G204700	*TaPAL5*	Cytoplasm	707	76,132.96	6.2107	−3.0	2D	156,707,284–156,709,989	F
6	TraesCS2B02G398400	*TaPAL6*	Cytoplasm	713	77,233.31	6.5058	0	2B	565,209,774–565,212,553	F
7	TraesCS1B02G048100	*TaPAL7*	Cytoplasm	714	77,341.05	5.9303	−6.5	1B	28,305,997–28,308,847	R
8	TraesCS2B02G224300	*TaPAL8*	Cytoplasm	706	76,220.04	6.3114	−2.0	2B	214,312,779–214,315,434	F
9	TraesCS2D02G377500	*TaPAL9*	Cytoplasm	713	77,188.05	5.9739	−5.5	2D	481,960,998–481,964,109	F
10	TraesCS4A02G401300	*TaPAL10*	Cytoplasm	713	77,087.87	6.1487	−4.0	4A	675,283,030–675,285,827	R
11	TraesCS1D02G039500	*TaPAL11*	Cytoplasm	714	77,180.97	6.3467	−2.0	1D	19,022,361–19,025,014	F
12	TraesCS2A02G380900	*TaPAL12*	Cytoplasm	713	77,261.17	6.1497	−4.0	2A	624,394,141–624,397,057	F
13	TraesCS5B02G468400	*TaPAL13*	Cytoplasm	552	58,944.16	6.5575	0.5	5B	641,833,347–641,835,469	F
14	TraesCS1D02G039400	*TaPAL14*	Cytoplasm	707	76,681.33	5.9509	−6.0	1D	19,012,091–19,020,939	R
15	TraesCS2D02G377600	*TaPAL15*	Cytoplasm	709	76,866.84	6.0796	−4.5	2D	481,988,232–481,990,914	F
16	TraesCS2D02G377200	*TaPAL16*	Cytoplasm	713	77,097.96	6.2412	−3.0	2D	481,599,475–481,602,192	F
17	TraesCS5B02G468300	*TaPAL17*	Cytoplasm	707	76,488.16	6.4644	−0.5	5B	641,822,078–641,824,730	F
18	TraesCS1B02G122800	*TaPAL18*	Cytoplasm	708	76,047.86	6.4086	−1.0	1B	148,413,936–148,416,442	R
19	TraesCS6D02G212500	*TaPAL19*	Cytoplasm	712	76,757.91	5.9498	−6.0	6D	300,896,671–300,900,381	R
20	TraesCS1B02G048200	*TaPAL20*	Cytoplasm	714	77,250.05	6.2977	−2.5	1B	28,322,038–28,324,849	R
21	TraesCS2A02G381100	*TaPAL21*	Cytoplasm	713	77,133.01	6.0528	−5.0	2A	624,458,106–624,460,956	F
22	TraesCS2B02G398000	*TaPAL22*	Cytoplasm	713	77,170.99	6.1485	−4.0	2B	564,920,332–564,923,399	F
23	TraesCS2B02G398200	*TaPAL23*	Cytoplasm	713	77,216.16	6.0265	−5.5	2B	565,076,277–565,079,194	F
24	TraesCS6A02G222700	*TaPAL24*	Cytoplasm	712	76,580.83	6.3123	−2.0	6A	416,648,337–416,650,876	F
25	TraesCS1A02G037700	*TaPAL25*	Cytoplasm	707	76,566.32	6.0782	−4.5	1A	20,924,887–20,932,614	R

Table 2. *Cont.*

Sr.#	Gene ID	Name	Subcellular Location	AA	MW (g/mol)	IP	Charge	Chrom	Gene Position Start–End (bp)	St
26	TraesCS6D02G212200	*TaPAL26*	Cytoplasm	704	75,619.36	6.211	−3.0	6D	300,326,934–300,333,023	R
27	TraesCS1D02G103500	*TaPAL27*	Cytoplasm	708	76,233.04	6.211	−3.0	1D	93,102,756–93,105,441	R
28	TraesCS6B02G258400	*TaPAL28*	Cytoplasm	704	75,605.29	6.1061	−4.0	6B	465,148,031–465,154,487	R
29	TraesCS1B02G048500	*TaPAL29*	Cytoplasm	714	77,314.11	6.096	−5.0	1B	28,483,566–28,486,349	F
30	TraesCS6D02G212400	*TaPAL30*	Cytoplasm	714	77,167.39	6.1081	−4.0	6D	300,888,767–300,893,342	R
31	TraesCS2B02G398100	*TaPAL31*	Cytoplasm	520	56,049.19	7.5761	8.5	2B	565,039,719–565,041,383	F
32	TraesCS6B02G258500	*TaPAL32*	Cytoplasm	714	77,108.33	6.2111	−3.0	6B	465,675,009–465,679,798	R
33	TraesCS1A02G037800	*TaPAL33*	Cytoplasm	714	77,228.05	6.3463	−2.0	1A	20,935,423–20,938,081	R
34	TraesCS2A02G380800	*TaPAL34*	Cytoplasm	713	77,015.89	6.2406	−3.0	2A	624,359,166–624,362,152	F
35	TraesCS2B02G224000	*TaPAL35*	Cytoplasm	707	76,207.83	5.7689	−7.0	2B	214,280,956–214,283,508	F
36	TraesCS2A02G196400	*TaPAL36*	Cytoplasm	668	71,935.46	7.4015	7.0	2A	166,254,570–166,256,576	F
37	TraesCS1A02G094900	*TaPAL37*	Cytoplasm	498	52,784.16	6.7764	2.0	1A	90,162,001–90,163,497	R

AA, amino acid; MW, molecular weight (g/mol); IP, isoelectric point; Chrom, chromosome; St, strand; R. reverse strand; F, forward strand.

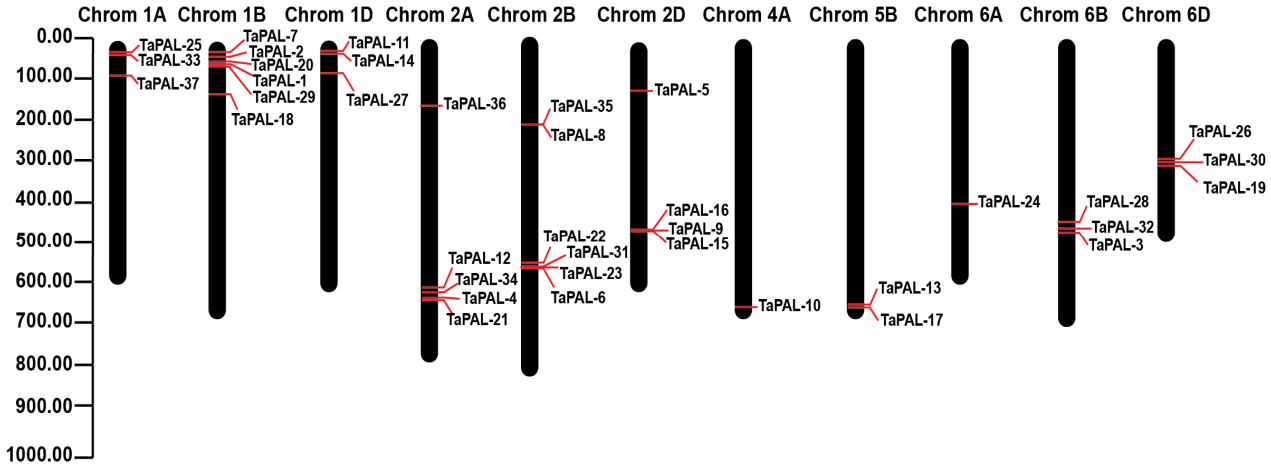

Figure 1. Localization of 37 *TaPAL* genes on wheat chromosomes. Each bar starts from the top, contains the chromosome number, and ends at the bottom. Genes numbers are according to Table 2. The size of the chromosome and the position of *TaPAL* are represented by the vertical scale in megabasepairs (Mb).

3.4. Gene Structure Analysis

For the determination of intron and exon numbers and their positions, all the coding and genomic sequences of *TaPAL* members were aligned. The analysis of *TaPAL* genes illustrated variations in exon–intron structure. Nine *TaPAL* genes (*TaPAL3*, *TaPAL5*, *TaPAL8*, *TaPAL18*, *TaPAL24*, *TaPAL27*, *TaPAL35*, *TaPAL36*, and *TaPAL37*) contained no introns in their ORFs (Figure 3). The present findings agreed with the previous studies, which reported that seven *CsPAL* genes contained no intron [26]. Parallel to our results, Vogt [5] also mentioned that none of the nine *ClPAL* genes contained introns. The ORFs of the 26 *TaPAL* genes (*TaPAL1-2*, *TaPAL4*, *TaPAL6-7*, *TaPAL9-12*, *TaPAL14-17*, *TaPAL20-23*, *TaPAL26*, and *TaPAL27-34*) were interrupted by a single intron (length ranged from 99 bp to 138 bp), whereas the intronic length of four genes (*TaPAL28*, *TaPAL32*, *TaPAL26* and *TaPAL30*) varied from 1055 bp to 1618 bp (Figure 3). Dong et al. [25] reported a similar exon–intron pattern in *AtPAL1* and *AtPAL2* [6], and *NtPALl*. Our results also explained that one additional intron was detected in *TaPAL25* and *TaPAL13*. Finally, the length of exon 2 was highly conserved in all the *TaPAL* genes with one intron.

3.5. Gene Ontology of PAL Genes

For the functional prediction of *PAL*-genes, we conducted GO annotation analysis. In silico functional prediction was carried out and results showed that there were three types of processes involved—biological processes (BPs), molecular processes (MPs), and cellular processes (CPs) (Figure 4). The BPs suggested that *PAL* genes are actively involved in the different metabolic activities and biosynthesis of different organic substances. Furthermore, CPs prediction clarified that almost all the *PAL* genes reside in the cytoplasm and could be involved in regulation of metabolic processes. Meanwhile, MPs showed that *PAL* genes have the enzymatic ability. Such findings clearly indicate that *PAL* genes play role in plant growth by modulating the BPs, MPs, and CPs.

3.6. MicroRNA-Targeting TaPAL Genes

We discovered 27 putative miRNAs targeting 37 *TaPAL* genes to create an interaction network using Cytoscape software to better understand the underlying regulatory mechanism of miRNAs involved in the regulation of *PALs* (Figure 5 and Supplementary Sheet S4). In the connection distribution and regulation network, we found that *TaPAL26* is one of the most-targeted *PAL* genes of wheat. The tae-miR1119 targets the wheat genes *TaPAL7*, *TaPAL32*, *TaPAL24*, *TaPAL3*, *TaPAL19*, *TaPAL30*, *TaPAL26*, *TaPAL27*, *TaPAL18*, *TaPAL9*,

TaPAL22, *TaPAL23*, *TaPAL21*, *TaPAL6*, *TaPAL16*, *TaPAL15*, *TaPAL33*, *TaPAL31*, and *TaPAL4*. Our results also indicated that miRNA tae-miR9781 target *TaPAL22* and *TaPAL34*. Both these genes have low expression in shoots. Furthermore, the miRNAs tae-miR1119, tae-miR398, tae-miR444a, tae-miR444b, and tae-miR9664-3p targeting *TaPAL29* have high expression in root tissues.

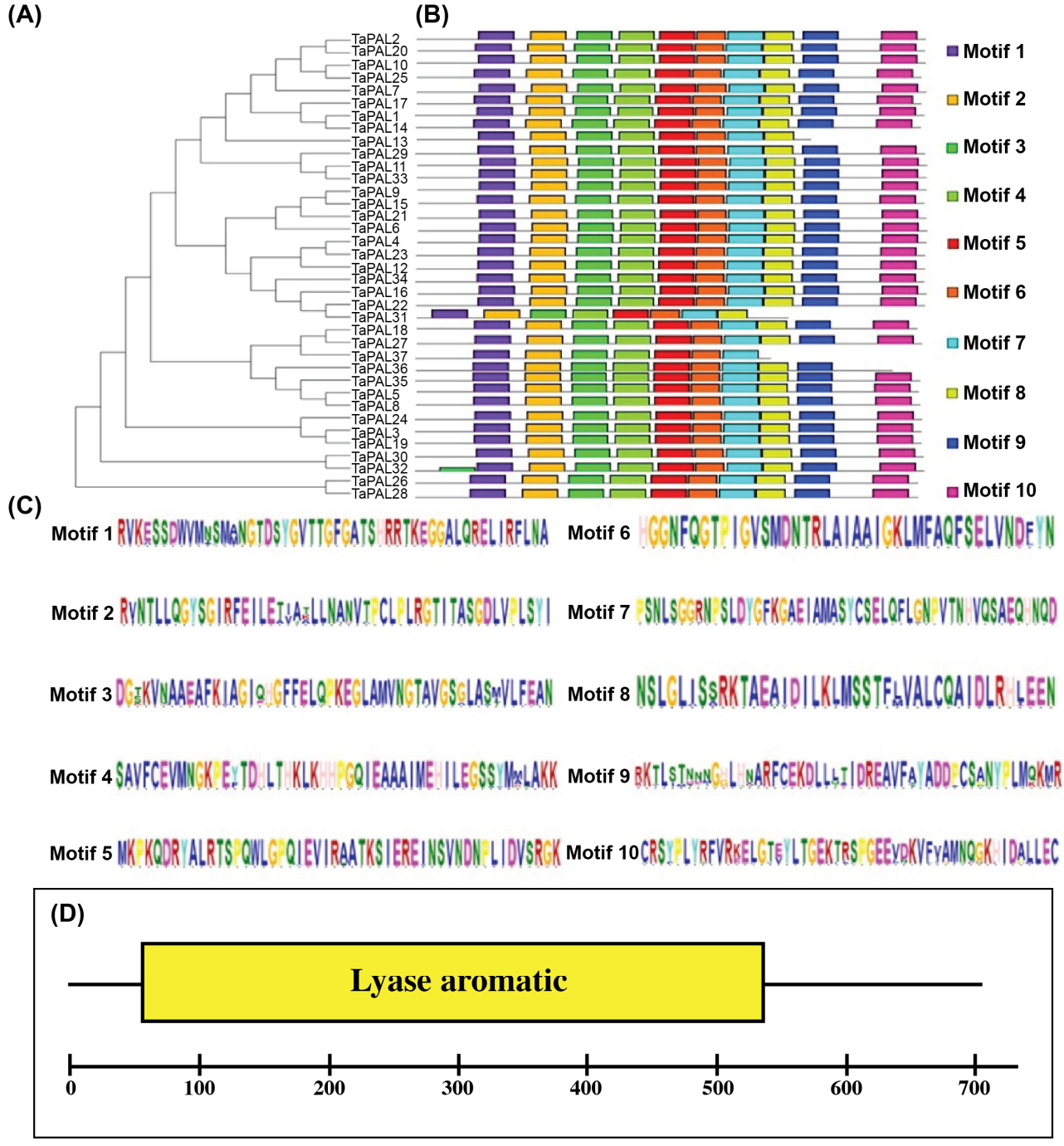

Figure 2. Phylogenetic tree and conserved domain analysis of *TaPAL* genes. (**A**) Thirty-seven TaPAL proteins sequences were used for the construction of phylogenetic tree, and 1000 replicates were also used for bootstrap test. (**B**) Ten conserve motifs with different lengths are shown. Motifs codes are presented at the right of the figure, with different colors. (**C**) Sequence logos of these motifs are presented. (**D**) Protein domain analysis showing the Pfam lyase aromatic domain.

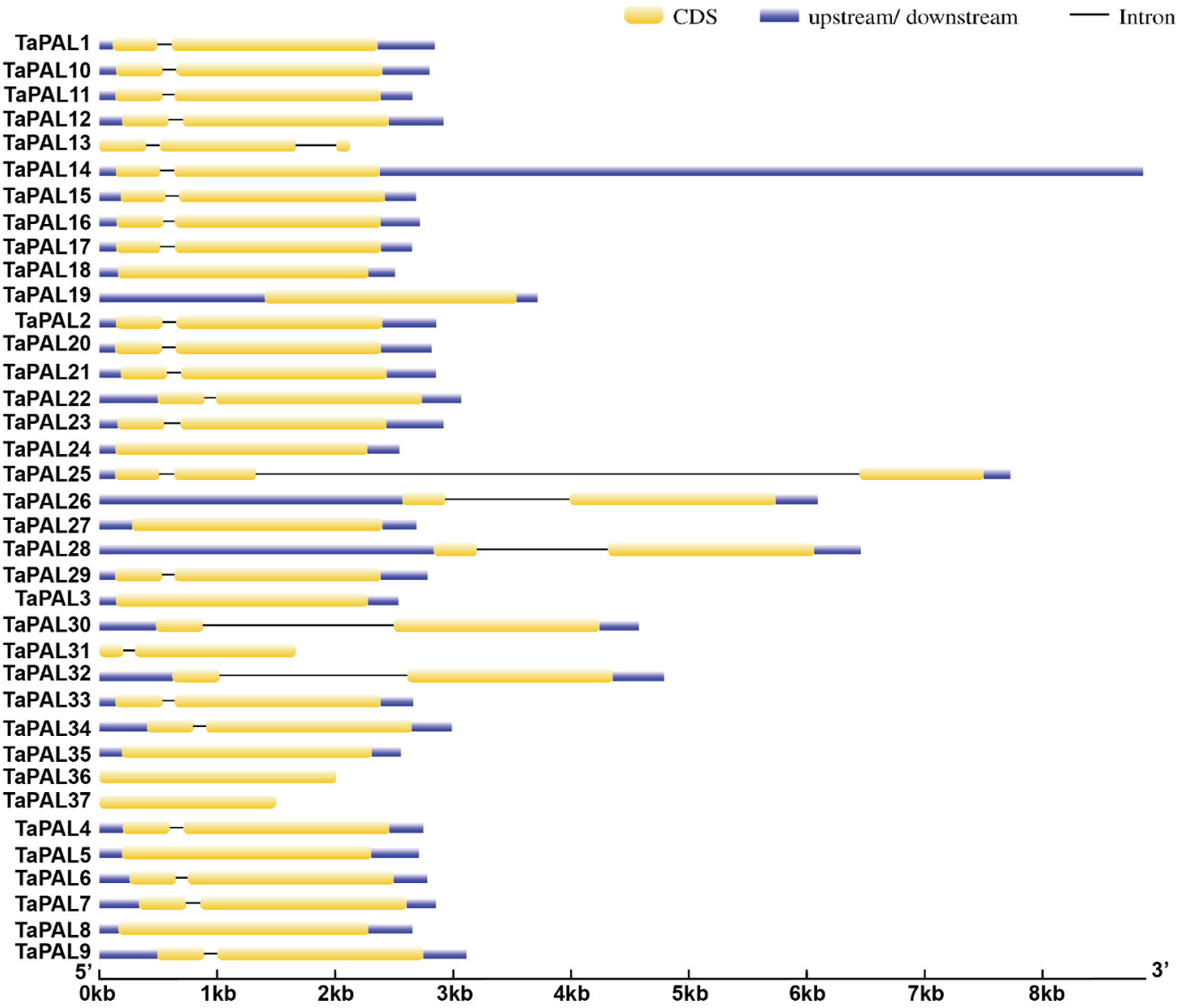

Figure 3. Gene structure analysis. Exon and intron arrangement-based gene structure of *TaPAL* genes.

3.7. Promoter Analysis

The promoter sequence is known as a regulatory element that controls gene expression and regulation [7–9]. The promoters are also called *cis*-acting regulatory DNA elements. Their location can be retrieved from the PLACE database (Table 3). Three regulatory elements, TCA-element, CGTAC-motif, and ABRE (abscisic acid or ABA responses), were identified for *TaPAL* genes. The TCA-element, CGTAC-motif, and ABRE-motifs are associated with SA responses, MeJA, and ABA, respectively.

Additionally, the expression of the *TaPAL* gene family is closely related to light, which was confirmed by the presence of MRE light-responsive element, G-Box, GT1-motif, AE-box, ATC-motif, C-box, CAG-motif, I-box, Sp1, Box 4, and ACE on some member *TaPAL* gene families. The putative TATA box was present on the upstream sequences from the start codon ATG on all *TaPAL* genes. Moreover, *TaPAL* gene promoters also contained several phytohormone-responsive elements, including ABRE, AuxRE (auxin-response elements), and GARE (gibberellin (GA) responses). The promoter of *TaPAL* genes also contained MBS (drought induction) and LTR repetitive sequences (cold stress) related to stress-response regulatory elements. *TaPAL21*, *TaPAL35*, *TaPAL8*, *TaPAL5*, *TaPAL16*, *TaPAL15*, *TaPAL28*, *TaPAL32*, *TaPAL26*, *TaPAL25*, *TaPAL18*, *TaPAL27*, *TaPAL36*, *TaPAL34*, and *TaPAL12* contained a single copy of MBS *cis*-regulatory element, while *TaPAL22* contained two

copies of MBS *cis*-regulatory element. It was also observed that only *TaPAL37*, *TaPAL29*, *TaPAL34*, *TaPAL35*, *TaPAL31*, *TaPAL24*, *TaPAL28*, *TaPAL3*, and *TaPAL19* contained the LTR *cis*-regulatory element. Additionally, the upstream regulatory sequences of the *TaPAL34* and *TaPAL16* genes contained the TC-rich repeat, which is related to the defense mechanism. These results suggested that the *TaPAL* gene family members may play an important role in the survival of plants under various environmental stresses. These *cis*-regulatory elements (promoters) receive stimuli from the environment via complex mechanisms and induce gene expression and regulation in response to various abiotic and biological stresses.

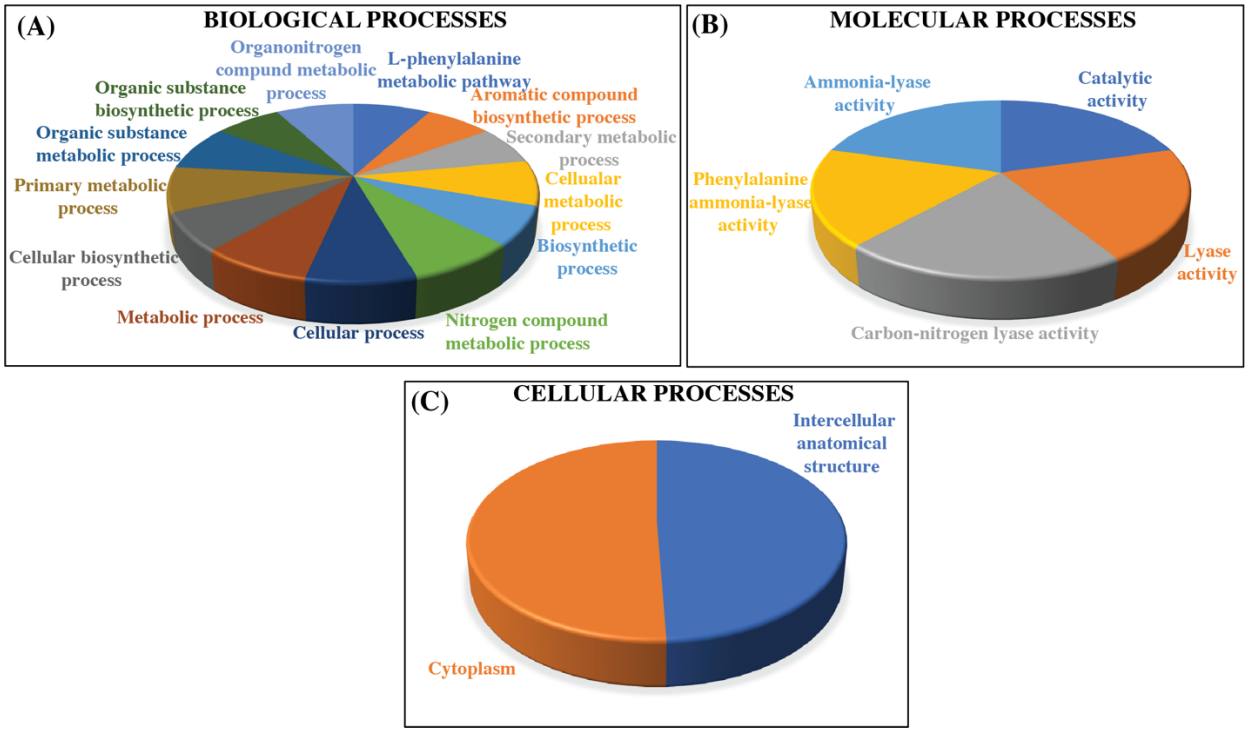

Figure 4. GO analysis of *PAL* genes. The data show (**A**) biological processes, (**B**) molecular processes, and (**C**) cellular processes.

3.8. Protein–Protein Interaction of TaPAL

The TaPAL protein predicted analysis showed an array of other proteins which co-regulate with TaPAL29 (Traes_1BS_BD86C90A7.1) (Figure 6). Arogenate dehydratase (Traes_5BL_7B0ED7548.1), which is a key enzyme involved in synthesis of L-phenylalanine from L-arogenate, showed interaction with our reference gene. The bit-score of 0.895 showed that optimum interaction with our reference gene TaPAL29, which is a member of the *TaPAL* genes, while rest of the gene was uncharacterized.

3.9. Phylogenetic Analysis of the PAL Gene Family

Of the 37 *TaPAL* genes identified in this study, four *PAL* genes from *Arabidopsis thaliana*, nine *PAL* genes from *Oryza sativa*, and eight *PAL* genes from *Zea mays* were used to construct a maximum-likelihood-approach tree using MEGA X to determine the evolutionary relationships (Figure 7). The resultant phylogenetic tree based on protein sequence similarities divided PAL proteins into four major clades or groups represented in different colors. The first three groups represent the monocots, while the fourth group shows the dicots. Overall group I exhibited 30 *TaPAL* genes (*TaPAL35-37*, *TaPAL1-2*, *TaPAL4-18*, *TaPAL20-23*, *TaPAL25*, *TaPAL27*, *TaPAL29*, TaPAL31, and *TaPAL33-37*) and one *PAL* gene from each rice and maize. Group II possessed five *TaPAL* genes (*TaPAL3*, *TaPAL19*, *TaPAL24*, *TaPAL30*, and *TaPAL32*) that were found to be more closely associated with the genes of *Z. mays* genes as compared to *O. sativa* genes. Moreover, group III illustrated two *TaPAL* genes (*TaPAL28* and *TaPAL26*) that were closely associated with *PAL* genes of *O. sativa* (*OsPAL1*, *OsPAL5*, and *OsPAL6*)

versus that of *Z. mays* (*ZmPAL1*). The *AtPALs* genes which are dicots and made a separate group IV.

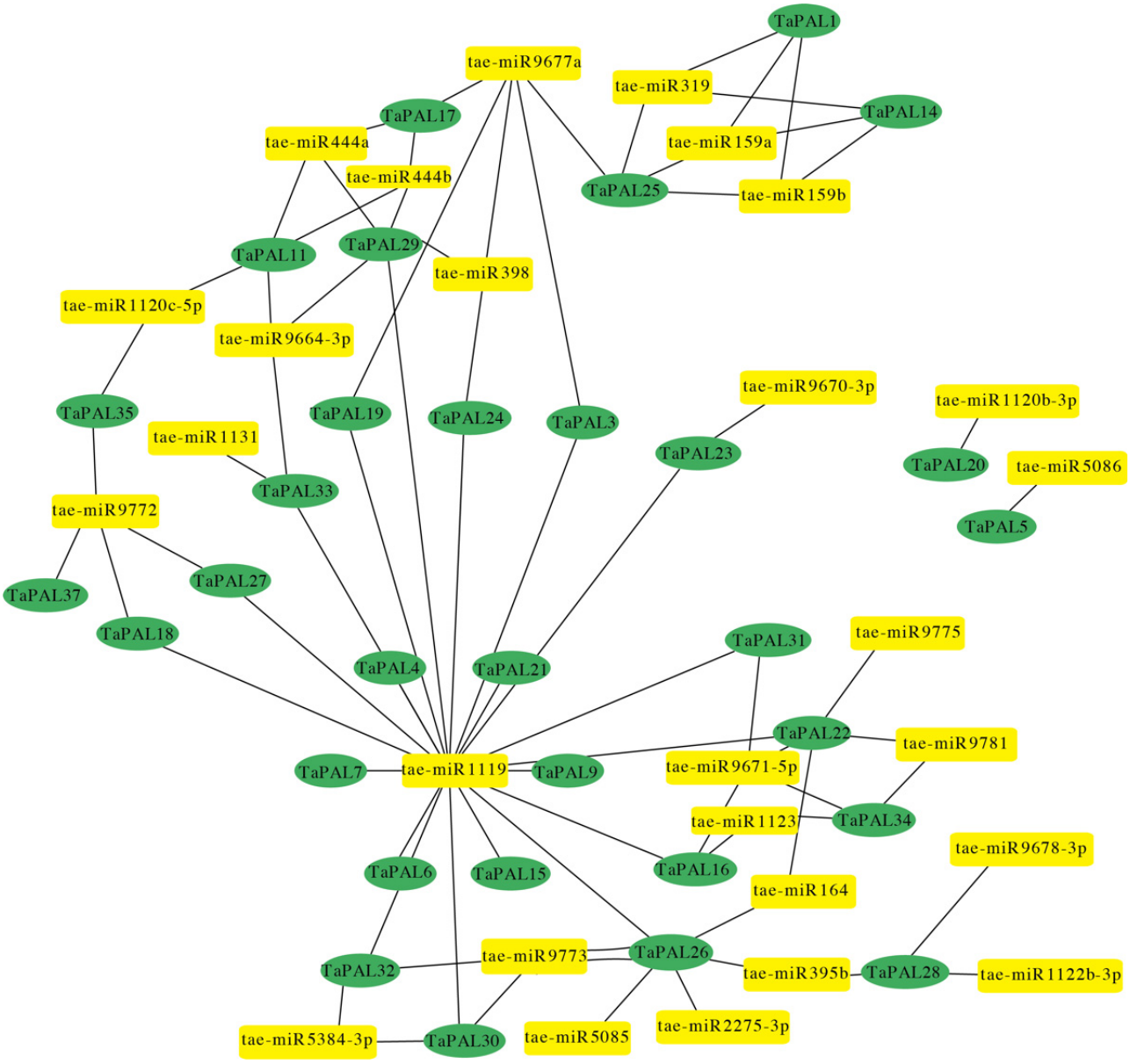

Figure 5. Regulatory network relationship between the miRNA and their targeted *TaPAL* genes.

Table 3. *Cis*-regulatory elements involved in plant growth regulation, stress, and hormonal responses.

	Site Name	Functions
Hormone	ABRE	*cis*-acting element involved in abscisic acid responsiveness
	ACE	*cis*-acting element involved in light responsiveness
	CCAAT-box	MYBHv1 binding site
	CGTCA-motif	*cis*-acting regulatory element involved in MeJA-responsiveness
	GARE-motif	Gibberellin-responsive element
	GC-motif	Enhancer-like element involved in anoxic-specific inducibility
	P-box	Gibberellin-responsive element and part of a light-responsive element
	TCA-element	*cis*-acting element involved in salicylic acid responsiveness
	TGA-element	Auxin-responsive element
	TGACG-motif	*cis*-acting regulatory element involved in MeJA-responsiveness

Table 3. *Cont.*

	Site Name	Functions
Stress and Growth	A-box	*cis*-acting regulatory element
	AE-box	Part of a module for light response
	Box 4	Part of a conserved DNA module involved in light responsiveness
	ARE	*cis*-acting regulatory element essential for anaerobic induction
	ATC-motif	Part of a conserved DNA module involved in light responsiveness
	ATCT-motif	Part of a conserved DNA module involved in light responsiveness
	C-box	*cis*-acting regulatory element involved in light responsiveness
	CAAT-box	Common *cis*-acting element in promoter and enhancer regions
	CAG-motif	Part of a light response element
	CAT-box	*cis*-acting regulatory element related to meristem expression
	chs-CMA2a	Part of a light responsive element
	chs-Unit 1 ml	Part of a light responsive element
	Circadian	*cis*-acting regulatory element involved in circadian control
	G-box	cis-acting regulatory element involved in light responsiveness
	GATA-motif	Part of a light-responsive element
	GCN4-motif	cis-regulatory element involved in endosperm expression
	GT1-motif	Light-responsive element
	GTGGC-motif	Part of a light-responsive element
	I-box	Part of a light-responsive element
	LTR	*cis*-acting element involved in low-temperature responsiveness
	MBS	MYB binding site involved in drought-inducibility
	O2-site	*cis*-acting regulatory element involved in zein metabolism regulation
	Sp1	Light-responsive element
	TATA-box	Core promoter element around -30 of transcription start
	TC-rich repeats	*cis*-acting element involved in defense and stress responsiveness
	TCT-motif	Part of a light responsive element

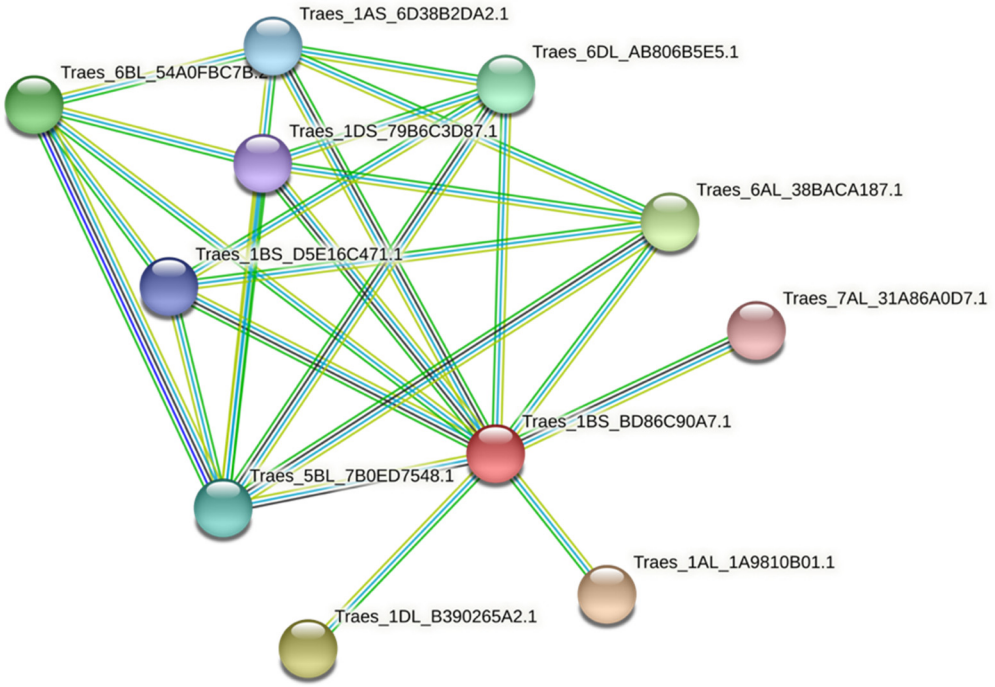

Figure 6. The predicted functional partners of TaPAL29.

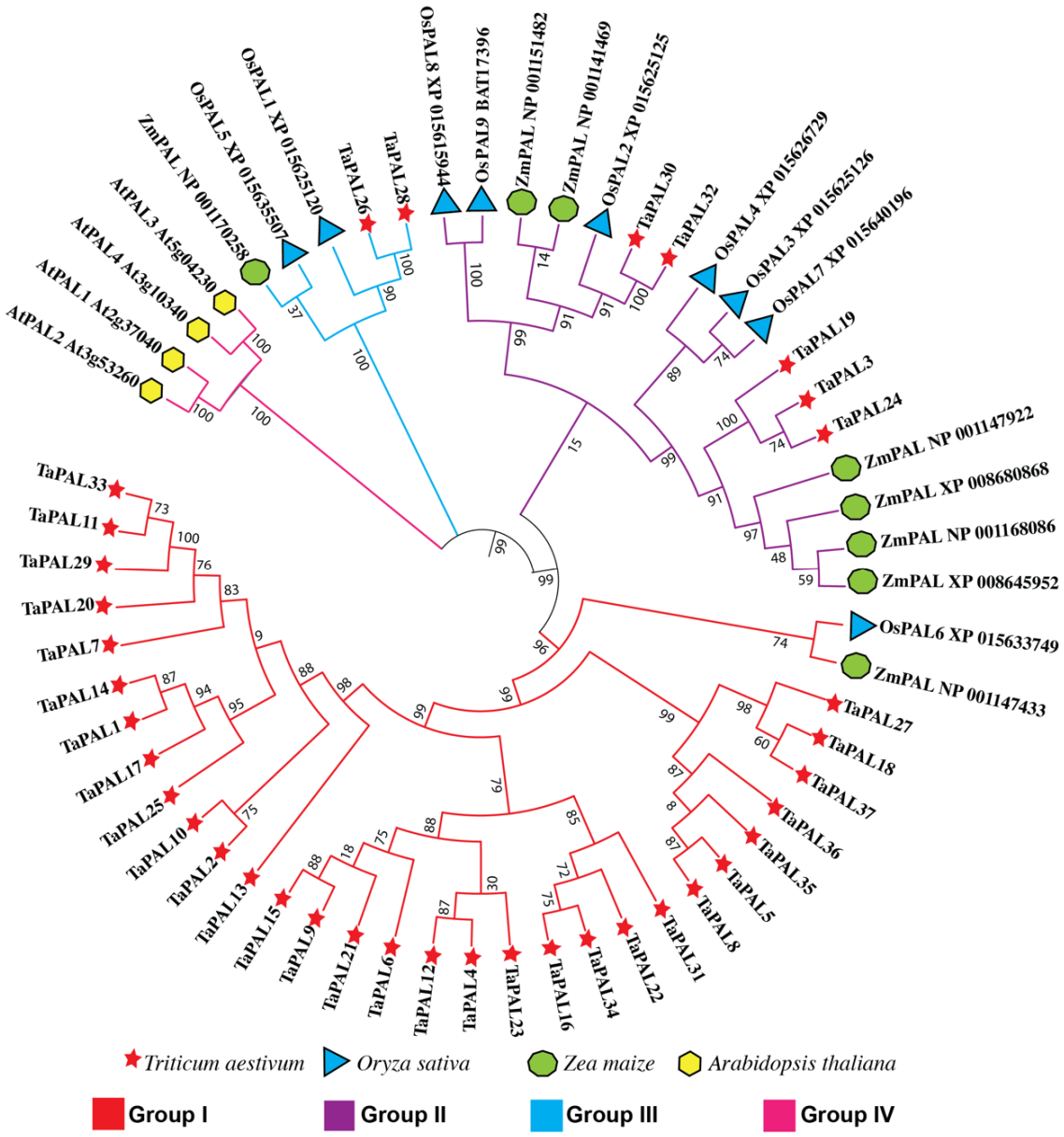

Figure 7. Comparative phylogenetic tree of PAL genes between *Triticum aestivum* (*Ta*), *Oryza sativa* (*Os*), *Zea maize* (*Zm*), and *Arabidopsis thaliana* (*At*). One thousand replicates were used for bootstrap test and the percentage of replication is presented next to the branches.

To investigate the ancestral relationship of the *PAL* gene family in *T. aestivum* with its ancestral species, the phylogenetic analysis also showed all the *PAL* genes from *Hordeum vulgare*, *Solanum tuberosum*, and *Triticum urartu*. *Hordeum vulgare* was domesticated from its wild relative, *Hordeum spontaneum*, while *Triticum urartu* is the progenitor of tetraploid *Triticum turgidum* and hexaploid *Triticum aestivum*. The ancestral plants had 8, 10, and 11 *PAL* genes, respectively. Common wheat *PAL* genes showed maximum association with *HvPAL* (*H. vulgare*), followed by *TuPAL* (*T. urartu*), as shown in Supplementary Figure S1.

To study the origin and evolutionary relationship of *Triticum aestivum* (*tr*), *Aegilops tauschii* (*ae*), *Triticum turgidum* (*tg*), and *Triticum dicocoides* (*td*) PAL protein sequences, a comparative synteny analysis was conducted (Figure 8 and Supplementary sheet S2). The proteins from four species were closely associated and showed higher similarity in evolutionary correlation analysis. It was noted that *TaPAL* genes on chromosome trchr6D have some evolutionary origins in common wheat with genes on chromosomes td6B, td6A, and ae6D. We identified that 10 genes of *Aegilops tauschii* are duplicated with *TaPAL33*,

TaPAL37, *TaPAL27*, *TaPAL34*, *TaPAL36*, *TaPAL22*, *TaPAL23*, *TaPAL35*, *TaPAL26*, and *TaPAL30*. Sixteen genes of *Triticum dicocoides* are orthologs with *TaPAL* genes of wheat, and *TaPAL26* is twice duplicated in *PAL* genes of *Triticum dicocoides*. Nineteen orthologous gene pairs of *Triticum turgidum* and wheat were identified. More than two of the orthologous gene pairs of *TaPAL 37*, *TaPAL36*, *TaPAL35*, *TaPAL34*, and *TaPAL26* were identified in *Triticum turgidum*. Seven paralogous pairs of *TaPAL* genes were identified.

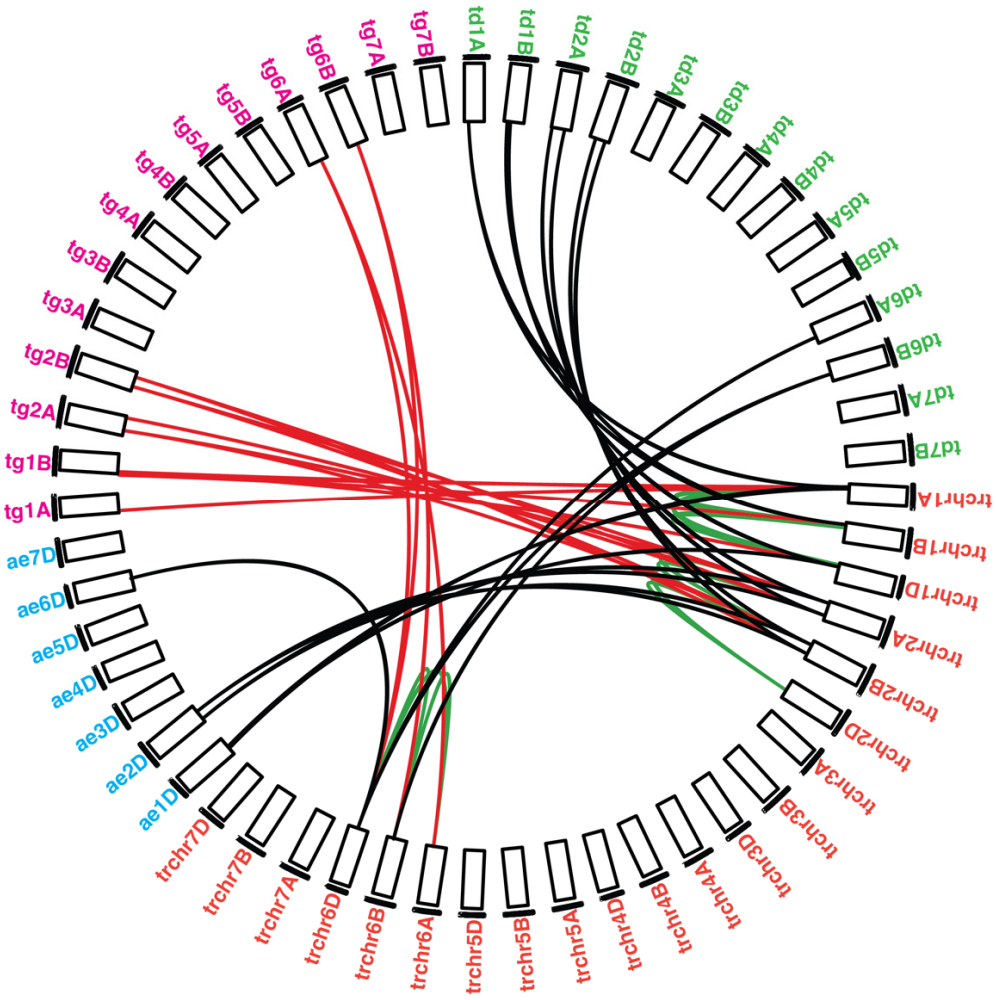

Figure 8. Evolutionary relationship of *PAL* genes between *Triticum aestivum* (*tr*, red), *Aegilops tauschii* (*ae*, blue), *Triticum turgidum* (*tg*, pink), and *Triticum dicocoides* (*td*, green). White bars represent chromosomes.

3.10. In Silico Expression Profile Analysis of PAL Gene Family in Six Genotypes of Wheat

Gene expression analysis helps to probe the potential role and functions of a gene family [57]. Comparative gene expression analysis was used to elucidate the physiological function of different *PAL* gene family members. The in-silico expression profiling was done on the roots of different wheat genotypes (Figure 9). For this purpose, RNA-seq-normalized data were analyzed and based on FPKM values, a heatmap was constructed for diverse *TaPAL* genes. The expression of *TaPAL* genes was variable in different wheat genotypes. *TaPAL35*, *TaPAL31*, *TaPAL23*, *TaPAL22*, *TaPAL8*, *TaPAL5*, and *TaPAL6* were only expressed in Local White. Very low expression of *TaPAL10*, *TaPAL30*, *TaPAL32*, *TaPAL3*, and *TaPAL28* were recorded in all wheat genotypes. Nonetheless, they may have tissue-specific expression, such as in seeds, or their expression may be induced only by certain environmental stresses. *TaPAL11*, *TaPAL14*, *TaPAL12*, *TaPAL34*, *TaPAL4*, *TaPAL21*, *TaPAL19*, *TaPAL24*, and *TaPAL36* were highly expressed in UZ-11-CWA-8. Similarly, *TaPAL27*, *TaPAL16*, *TaPAL9*, and *TaPAL15* were highly expressed in Chakwal-50. Overall, *TaPAL* genes showed a higher expression

pattern in roots of drought-tolerant genotypes as compared to drought-sensitive genotypes of wheat.

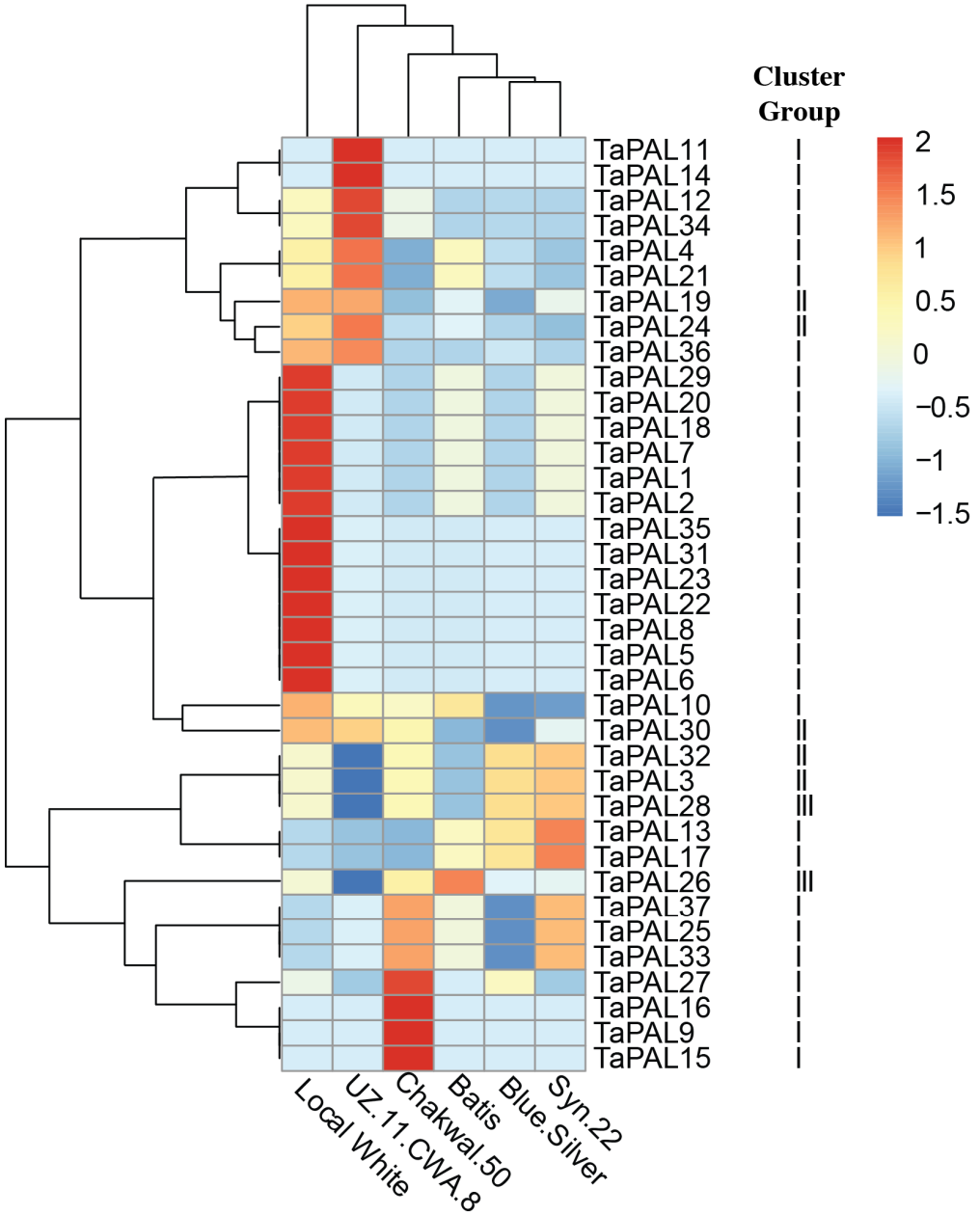

Figure 9. Heatmap of expression pattern of *TaPAL* genes in roots of different wheat genotypes based on FPKM values. Cluster grouping shown as in Figure 7. Color scheme showing the intensity of expression (blue, low expression; red, high expression, and Z score was used).

3.11. Expression of PAL Gene Family under Abiotic Stress

The expression of *TaPAL* genes under abiotic stresses such as drought (DH), heat stress (HS), and phosphorous deficiency (PS) at various stages and in various tissues were explored (Figure 10 and Supplementary Sheet S3). The expression levels of *TaPAL37*, *TaPAL36*, *TaPAL35*, *TaPAL33*, *TaPAL29*, *TaPAL25*, *TaPAL24*, *TaPAL17*, *TaPAL14*, *TaPAL11*, *TaPAL7*, *TaPAL3*, and *TaPAL4* were upregulated in roots. Similarly, the same trend was shown by *TaPAL10*, *TaPAL27*, *TaPAL15*, *TaPAL6*, and *TaPAL21* under drought stress, while *TaPAL23*, *TaPAL20*, *TaPAL19*, *TaPAL2*, and *TaPAL13* were regulated non-significantly under all conditions.

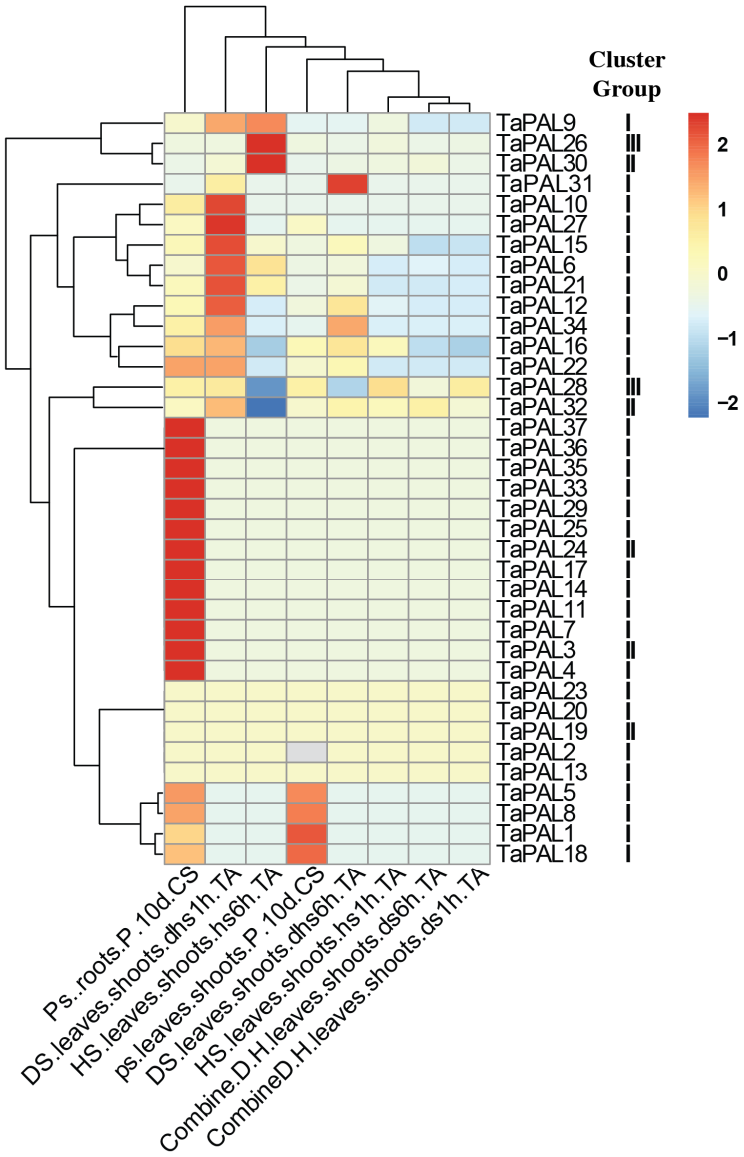

Figure 10. Expression profile of *TaPAL* genes under abiotic stresses. Cluster grouping shown as in Figure 7. Expression values are represented by color scale. Red and blue colors represent the gene expression of up-regulated and down-regulated genes, respectively; yellow shows expression was unregulated. Details are presented in Supplementary Sheet S1.

4. Discussion

Wheat is the main crop for half of the world's population. Wheat faces various types of biotic and abiotic stresses. It has been suggested that *phenylalanine ammonia-lyase (PAL)* genes are essential for plant growth, development, adaptation, and mitigation responses to various environmental and pathogens stresses by producing secondary metabolites regulating plant growth response [11,58,59]. Phenylpropanoids are plant-based organic compounds, which are produced from the amino acids phenylalanine and tyrosine. PAL serves as the first enzyme in the phenylpropanoid pathway and in flavonoid biosynthesis that catalyzes the deamination of phenylalanine [1,24,45,60,61]. Recently, these enzymes have been reported by many researchers in different crops, including *Juglans regia* [62], *Citrus reticulata* [63], *Citrullus lanatus* [64], and *Medicago truncatula* [65]. This study was an investigation of *PAL* in wheat.

The *PAL* family is a very large, multigene family. The family includes ten putative members in maize [66], four members in *Arabidopsis* [19] and tobacco [67], and more than

20 copies in tomato and potato [68]. In the present study, we demonstrated that common wheat (*Triticum aestivum*) has 37 genes of the *PAL* family, a significantly higher number than the above-mentioned species. However, the increase and decrease of *PAL* genes present among species (*Z. mays*, *A. thaliana*, and *O. sativa)* is random [6]. Our results showed that the number of *PAL* genes in *T. aestivum* far exceeds the four *AtPALs*, seven *OsPALs*, twelve *JrPALs*, and six *ZmPALs*, suggesting that whole-genome duplication, small-scale segmental duplications, local tandem duplications, or a combination of these duplication events may have caused this expansion in *T. aestivum* [7,69,70]. The duplicated *PAL* genes in this study were mapped to 11 chromosomes (Figure 1). This diversity of chromosomal distribution indicates that these genes have diverse function. The duplication events might have caused the expansion and dispersion of *PAL* genes giving rise to potential sources of functional variability in common wheat. Gene duplication events may have caused the significant increase in *PAL* genes in *T. aestivum*, as stated in recent studies on different species [16,42,65]. The isolation and identification of *PAL* genes in *T. aestivum* is critical because of their importance in adaption and stress resistance [1,71,72]. The activity of *PAL* genes in response to cold stress of *Juglans regia* (walnut) suggested that the *PAL* gene family in *T. aestivum* is also involved in providing resistance against cold, drought, salt, and disease [70,72]. Similarly, this study also indicates that the expression of *TaPAL* genes is higher in drought-tolerant wheat genotypes as compared to sensitive genotypes. Furthermore, we also checked the subcellular location of TaPAL. Our results showed that the 37 PAL genes are localized to the cytoplasm [62,73,74].

Conserved motifs referred to a part of proteins that is functionally important. The motifs were selected from the PLACE database and conservation patterns were retrieved from MEME suite (Figure 2 and Table 3) and UGENE depicted that the protein structure of the *PAL*-gene family has been highly conserved. The *PAL*-gene family, including *Z. mays*, *A. thaliana*, *O. sativa*, *H. vulgare*, and *T. urartu* plant species, contained all the conserved domains indicating that the *PAL*-gene family remained highly conserved during evolution and took long-term speciation and duplication events to evolve; thus, the results demonstrated its importance in antiretroviral effects. It was evident that the key domain is phenyl ammonium lyase/aromatic lyase, which exists in all families and ancestral species, suggesting a structural similarity between proteins of the *PAL* gene family.

The intron–exon gene structure gives clues for gene evolution [10]. In parallel to the gene number, the structure of the *TaPAL* genes in *Triticum aestivum* has experienced developmental/evolutionary modifications. Out of 37 *TaPAL* genes, ten *TaPAL* genes (*TaPAL3*, *TaPAL5*, *TaPAL8*, *TaPAL18*, *TaPAL19*, *TaPAL24*, *TaPAL27*, *TaPAL35*, *TaPAL36*, and *TaPAL37*) have no intron in their coding regions, two of the *TaPAL* genes (*TaPAL25*, and *TaPAL13*) are interrupted by two introns in their ORFs, while 25 *TaPAL* genes have one intron in their ORFs (Figure 3). Recent studies stated that the duplicated genes showed structural divergence, which is very prevalent in the generation of functionally distinct paralogs. This structural divergence has played a key role in the evolution of duplicated genes compared to non-duplicated genes [69]. The *PAL*-gene structural-data analysis showed a significant variation in the evolution of the *PAL* family of common wheat, walnut, and poplar.

For the functional prediction of *TaPAL* genes we did the GO enrichment analysis (Figure 4). In silico prediction indicated that *TaPAL* genes were involved in numerous developmental processes by regulating biological processes (BPs), molecular processes (MPs), and cellular process (CPs), and showed response against environmental stresses. Many previous studies also reported that microRNAs respond to stress stimuli through regulation of gene expression [42]. *TaPAL* is highly expressed in roots as compared to shoot tissues against abiotic stress. The miRNAs tae-miR1119, tae-miR398, tae-miR444a, tae-miR444b, and tae-miR9664-3p targeting *TaPAL29* have high expression in root tissues (Figures 5 and 10). Previously it has been reported that plant miRNAs play a role in response to environmental stress. In bread wheat under the drought stress, different miRNAs such as miR159, and miR395 were found to be differentiated [75]. Similarly, *VM-*

milR37 plays role in pathogenicity through regulation of the *VmGPX* gene [76]. In another study, miR164 regulated the salinity tolerance in maize [77]. We also checked the protein–protein interaction of TaPAL29 with other co-regulated proteins. Results showed that arogenate dehydratase belongs to the class lyases and is a key enzyme that catalyzes the reaction of L-arogenate into L-phenylalanine [78] and shows interaction with the TaPAL29 (Figure 6).

Phylogenetic analysis, both with ancestral and family species, proposed that the evolution trajectories are like family species (*Z. mays*, *A. thaliana*, and *O. sativa)* and suggested that the *PAL* gene family converge to a single ancestor. This ancestor might be involved in the evolution of plants with respect to adaptation and resistance. Previously it has been reported that during the evolution of PAL, lineage-specific duplication (to promote the diversity of multi-gene families) occurs in *Arabidopsis* and other species [79]. The close paralogs of each PAL gene clustered together phylogenetically into clades in *T. aestivum*, *A. thaliana*, *O. sativa*, and *Z. mays* (Figure 7). In contrast, the PALs from *T. aestivum* and *Z. mays* clustered together along with some of the *O. sativa* genes (*OsPAL1*, *OsPAL5*, *OsPAL6*, and *OsPAL8*), indicating that the expansion of the common wheat PAL gene family might have occurred after the divergence of eurosids I and eurosids II (approximately 100 million years ago) which was reported by [62,80]. Based on phylogenetic analysis, our 37 *TaPAL* genes were separated into three different groups as in tea plant (*Camellia sinensis)* [79] and in other woody plants (*Juglans regia* L., *Salix babylonica*, *Ornithogalum saundersiae*, and *Populus trichocarpa*) they cluster into two groups [18,21,42,81]. TaPALs showed no expansion events as in *Cucumis sativus* [26]. The *PAL* gene family has significant similarities and dissimilarities among various plant species, i.e., *ZmPAL3-5* and *OsPAL2-4*. Among *TaPAL* genes, *TaPAL13*, *TaPAL31*, *TaPAL36*, and *TaPAL37* showed a slight difference in sequence as compared to other 33 *PAL* genes of *T. aestivum* (common wheat), which indicated an 80% similarity score in syntenic analysis. This relationship demonstrated that PALs with comparable evolutionary status might play a similar role in plant development, which enabled us to examine the elements of PALs from different families such as Poaceae via utilizing a comparative genomic approach.

PAL gene is strictly involved in controlling the pre- and post-transcriptional stages, which is considered a doorway to the initiation of the phenylpropanoid pathway. Differential expression patterns for *PAL* genes in higher plants was observed. Moreover, the *PAL* genes in common wheat (*T. aestivum*) show distinct patterns of expression in roots. The genes *TaPAL11*, *TaPAL14*, *TaPAL12*, *TaPAL29*, *TaPAL20*, *TaPAL7*, *TaPAL1*, *TaPAL2*, *TaPAL9*, *TaPAL15,* and *TaPAL16* exhibited high expression levels in roots of drought-tolerant genotypes as compared to drought-susceptible genotypes (Figure 9). These variations in expression level were attributed to the differences in proteins and gene structures, as shown in Figures 2 and 3. The *PAL* family genes showed diverse expression patterns, which indicated that a complex regulation of the PAL-mediated phenylpropanoid pathways existed during the development of drought-tolerant and drought-sensitive wheat genotypes (Figure 9). A similar expression pattern of the *PAL* gene family has also been reported in walnut and barrel clover [62,82]. *Cis*-regulatory elements are also present upstream of the TaPALs (Table 3). Some of the TaPALs from the same evolutionary cluster co-express under stress conditions. This might be due to the presence of *Cis* elements [16]. Similarly, *GdPAL5* is also reported to be an auxin producer which activates plant defense mechanisms during the abiotic stress [83]. Different gene family members usually display abundance disparities in different tissues or under distinct stresses [84].

To overcome the problem of changing climatic conditions of abiotic stress including heat and drought stress on wheat, there is a need to explore the transcriptome profile of this gene family. This study used transcriptomic information of various tissues, at various stages, as shown in Figure 10. The transcript levels of *TaPAL37*, *TaPAL36*, *TaPAL35*, *TaPAL33*, *TaPAL29*, *TaPAL25*, *TaPAL24*, *TaPAL17*, *TaPAL14*, *TaPAL11*, *TaPAL7*, *TaPAL3*, and *TaPAL4* were upregulated in roots. The expression levels of *TaPAL* genes were consistent with previous studies, showing that expression of *TaPAL* genes is higher in roots as compared to

other tissues of plants such as *Hordeum vulagare* [85], *Solanum tuberosum* [86], *Arabidopsis thaliana* [19], and *Juglans regia* [87]. The higher expression of the *TaPAL* gene family in drought-tolerant genotypes as compared to drought-sensitive genotypes may be due to high level of lignification, which is part of normal root development [88]. Furthermore, publicly available transcriptomic data which we used was validated by qRT-PCR [89,90].

5. Conclusions

In this study, we have identified 37 *TaPAL* gene family members, which were distributed onto 11 chromosomes. These *TaPAL* genes were found to be involved in drought-stress response mechanisms as they showed high expression in root tissues. Since a few *PAL* genes are reported in wheat, this is the first detailed study of the *PAL* gene family in wheat. We also find 27 putative miRNAs targeting *TaPAL* genes. Some questions are still to be answered, such as what is the exact role of each *TaPAL* gene, and how is the expression of each *TaPAL* controlled in different phases of development and in reaction to distinct stress or hormone signals? Therefore, to further our knowledge of the *TaPAL* family, more molecular, biochemical, and physiological studies are expected. Due to the potential roles of *TaPAL* in the growth of common wheat (*T. aestivum*), it may provide prospective targets for molecular high-quality grain breeding.

Supplementary Materials: The following are available online at https://www.mdpi.com/article/10.3390/agronomy11122511/s1, Figure S1: Ancestral relationship (phylogenetic tree) of *PAL* genes between *Triticum aestivum (Ta)*, *Hordeum vulgare (Hv)*, *Solanum tuberosum (St)*, and *Triticum urartu (Tu)*; File S1: Protein sequences of identified TaPAL in this study; File S2: Multiple sequence alignment in wheat; Supplementary Sheet S1:The details of the materials and treatments for the retrieved expression values; Sheet S2:List of genes in wheat to explore the gene duplication within the TaPAL gene family and ancestral species of wheat; Sheet S3: Expression level of genes in different conditions; Sheet S4:Putative miRNAs targeting the *TaPAL* genes.

Author Contributions: Conceptualization, F.R. and M.R.K.; data curation, F.R., M.U., M.K.N., N.R., A.A. and H.S.; formal analysis, F.R. and N.R.; funding acquisition, M.R.K.; methodology, M.R.K.; resources, M.R.K.; software, F.R.; supervision, M.R.K.; validation, M.U. and M.R.K.; visualization, M.U.; writing—original draft, F.R.; writing—review and editing, F.R., M.U. and M.R.K. All authors have read and agreed to the published version of the manuscript.

Funding: This research was funded by ALP, PARC, Pakistan.

Institutional Review Board Statement: Not applicable.

Informed Consent Statement: Not applicable.

Data Availability Statement: The data and materials presented in this study are mentioned in the main text as well as in the supplementary files, further data will be provided on request from the corresponding author.

Acknowledgments: We acknowledge the assistance of NIGAB, NARC, Islamabad, Pakistan for infrastructural support.

Conflicts of Interest: The authors declare no conflict of interest. The funders had no role in the design of the study; in the collection, analyses, or interpretation of data; in the writing of the manuscript, or in the decision to publish the results.

References

1. Huang, J.; Gu, M.; Lai, Z.; Fan, B.; Shi, K.; Zhou, Y.-H.; Yu, J.-Q.; Chen, Z. Functional analysis of the Arabidopsis *PAL* gene family in plant growth, development, and response to environmental stress. *Plant Physiol.* **2010**, *153*, 1526–1538. [CrossRef] [PubMed]
2. Wu, P.; Guo, Q.-q.; Qin, Z.-w. The fungicide propamocarb increases lignin by activating the phenylpropanoid pathway in *Cucumis sativus* L. *Hortic. Environ. Biotechnol.* **2016**, *57*, 511–518. [CrossRef]
3. Raza, A.; Su, W.; Hussain, M.A.; Mehmood, S.S.; Zhang, X.; Cheng, Y.; Zou, X.; Lv, Y. Integrated Analysis of Metabolome and Transcriptome Reveals Insights for Cold Tolerance in Rapeseed (*Brassica napus* L.). *Front. Plant Sci.* **2021**, *12*, 1796. [CrossRef]
4. Schwede, T.F.; Rétey, J.; Schulz, G.E. Crystal structure of histidine ammonia-lyase revealing a novel polypeptide modification as the catalytic electrophile. *Biochemistry* **1999**, *38*, 5355–5361. [CrossRef]

5. Vogt, T. Phenylpropanoid biosynthesis. *Mol. Plant* **2010**, *3*, 2–20. [CrossRef] [PubMed]
6. Cochrane, F.C.; Davin, L.B.; Lewis, N.G. The Arabidopsis phenylalanine ammonia lyase gene family: Kinetic characterization of the four PAL isoforms. *Phytochemistry* **2004**, *65*, 1557–1564. [CrossRef]
7. Pascual, M.B.; El-Azaz, J.; de la Torre, F.N.; Cañas, R.A.; Avila, C.; Cánovas, F.M. Biosynthesis and metabolic fate of phenylalanine in conifers. *Front. Plant Sci.* **2016**, *7*, 1030. [CrossRef]
8. Lei, L.; Zhou, S.-L.; Ma, H.; Zhang, L.-S. Expansion and diversification of the SET domain gene family following whole-genome duplications in *Populus trichocarpa*. *BMC Evol. Biol.* **2012**, *12*, 1–17. [CrossRef]
9. Dixon, R.A.; Paiva, N.L. Stress-induced phenylpropanoid metabolism. *Plant Cell* **1995**, *7*, 1085. [CrossRef]
10. La Camera, S.; Gouzerh, G.; Dhondt, S.; Hoffmann, L.; Fritig, B.; Legrand, M.; Heitz, T. Metabolic reprogramming in plant innate immunity: The contributions of phenylpropanoid and oxylipin pathways. *Immunol. Rev.* **2004**, *198*, 267–284. [CrossRef]
11. Kim, D.S.; Hwang, B.K. An important role of the pepper phenylalanine ammonia-lyase gene (PAL1) in salicylic acid-dependent signalling of the defence response to microbial pathogens. *J. Exp. Bot.* **2014**, *65*, 2295–2306. [CrossRef] [PubMed]
12. Ritter, H.; Schulz, G.E. Structural basis for the entrance into the phenylpropanoid metabolism catalyzed by phenylalanine ammonia-lyase. *Plant Cell* **2004**, *16*, 3426–3436. [CrossRef]
13. Purwar, S.; Sundaram, S.; Sinha, S.; Gupta, A.; Dobriyall, N.; Kumar, A. Expression and in silico characterization of Phenylalanine ammonium lyase against karnal bunt (*Tilletia indica*) in wheat (*Triticum aestivum*). *Bioinformation* **2013**, *9*, 1013. [CrossRef] [PubMed]
14. Rawal, H.; Singh, N.; Sharma, T. Conservation, divergence, and genome-wide distribution of *PAL* and *POX* A gene families in plants. *Int. J. Genom.* **2013**, *2013*, 678969.
15. MacDonald, M.J.; D'Cunha, G.B. A modern view of phenylalanine ammonia lyase. *Biochem. Cell Biol.* **2007**, *85*, 273–282. [CrossRef] [PubMed]
16. Wu, Z.; Gui, S.; Wang, S.; Ding, Y. Molecular evolution and functional characterisation of an ancient phenylalanine ammonia-lyase gene (*NnPAL1*) from *Nelumbo nucifera*: Novel insight into the evolution of the PAL family in angiosperms. *BMC Evol. Biol.* **2014**, *14*, 1–14. [CrossRef]
17. Chaw, S.-M.; Zharkikh, A.; Sung, H.-M.; Lau, T.-C.; Li, W.-H. Molecular phylogeny of extant gymnosperms and seed plant evolution: Analysis of nuclear 18S rRNA sequences. *Mol. Biol. Evol.* **1997**, *14*, 56–68. [CrossRef]
18. de Jong, F.; Hanley, S.J.; Beale, M.H.; Karp, A. Characterisation of the willow phenylalanine ammonia-lyase (PAL) gene family reveals expression differences compared with poplar. *Phytochemistry* **2015**, *117*, 90–97. [CrossRef]
19. Wanner, L.A.; Li, G.; Ware, D.; Somssich, I.E.; Davis, K.R. The phenylalanine ammonia-lyase gene family in *Arabidopsis thaliana*. *Plant Mol. Biol.* **1995**, *27*, 327–338. [CrossRef]
20. Raes, J.; Rohde, A.; Christensen, J.H.; Van de Peer, Y.; Boerjan, W. Genome-wide characterization of the lignification toolbox in Arabidopsis. *Plant Physiol.* **2003**, *133*, 1051–1071. [CrossRef]
21. Shi, R.; Sun, Y.-H.; Li, Q.; Heber, S.; Sederoff, R.; Chiang, V.L. Towards a systems approach for lignin biosynthesis in *Populus trichocarpa*: Transcript abundance and specificity of the monolignol biosynthetic genes. *Plant Cell Physiol.* **2010**, *51*, 144–163. [CrossRef] [PubMed]
22. Xu, H.; Park, N.I.; Li, X.; Kim, Y.K.; Lee, S.Y.; Park, S.U. Molecular cloning and characterization of phenylalanine ammonia-lyase, cinnamate 4-hydroxylase and genes involved in flavone biosynthesis in *Scutellaria baicalensis*. *Bioresour. Technol.* **2010**, *101*, 9715–9722. [CrossRef] [PubMed]
23. Lepelley, M.; Mahesh, V.; McCarthy, J.; Rigoreau, M.; Crouzillat, D.; Chabrillange, N.; de Kochko, A.; Campa, C. Characterization, high-resolution mapping and differential expression of three homologous PAL genes in *Coffea canephora* Pierre (Rubiaceae). *Planta* **2012**, *236*, 313–326. [CrossRef] [PubMed]
24. Bagal, U.R.; Leebens-Mack, J.H.; Lorenz, W.W.; Dean, J.F. The phenylalanine ammonia lyase (PAL) gene family shows a gymnosperm-specific lineage. In *Proceedings of the BMC Genomics*; Springer: Berlin/Heidelberg, Germany, 2012; pp. 1–9.
25. Dong, C.-j.; Ning, C.; ZHANG, Z.-g.; SHANG, Q.-m. Phenylalanine ammonia-lyase gene families in cucurbit species: Structure, evolution, and expression. *J. Integr. Agric.* **2016**, *15*, 1239–1255. [CrossRef]
26. Shang, Q.-M.; Li, L.; Dong, C.-J. Multiple tandem duplication of the phenylalanine ammonia-lyase genes in *Cucumis sativus* L. *Planta* **2012**, *236*, 1093–1105. [CrossRef]
27. Souri, Z.; Karimi, N.; Sandalio, L.M. Arsenic hyperaccumulation strategies: An overview. *Front. Cell Dev. Biol.* **2017**, *5*, 67. [CrossRef]
28. Bolser, D.; Staines, D.M.; Pritchard, E.; Kersey, P. Ensembl plants: Integrating tools for visualizing, mining, and analyzing plant genomics data. In *Plant Bioinformatics*; Springer: Berlin/Heidelberg, Germany, 2016; pp. 115–140.
29. Madden, T. The BLAST sequence analysis tool. In *NCBI Handbook*, 2nd ed.; National Center for Biotechnology Information (US): Bethesda, MD, USA, 2013; Volume 2, pp. 425–436.
30. Larkin, M.A.; Blackshields, G.; Brown, N.P.; Chenna, R.; McGettigan, P.A.; McWilliam, H.; Valentin, F.; Wallace, I.M.; Wilm, A.; Lopez, R. Clustal W and Clustal X version 2.0. *Bioinformatics* **2007**, *23*, 2947–2948. [CrossRef]
31. Bateman, A.; Coin, L.; Durbin, R.; Finn, R.D.; Hollich, V.; Griffiths-Jones, S.; Khanna, A.; Marshall, M.; Moxon, S.; Sonnhammer, E.L. The Pfam protein families database. *Nucleic Acids Res.* **2004**, *32*, D138–D141. [CrossRef]
32. Schultz, J.; Copley, R.R.; Doerks, T.; Ponting, C.P.; Bork, P. SMART: A web-based tool for the study of genetically mobile domains. *Nucleic Acids Res.* **2000**, *28*, 231–234. [CrossRef]

33. Hu, B.; Jin, J.; Guo, A.-Y.; Zhang, H.; Luo, J.; Gao, G. GSDS 2.0: An upgraded gene feature visualization server. *Bioinformatics* **2015**, *31*, 1296–1297. [CrossRef]
34. Bailey, T.L.; Boden, M.; Buske, F.A.; Frith, M.; Grant, C.E.; Clementi, L.; Ren, J.; Li, W.W.; Noble, W.S. MEME SUITE: Tools for motif discovery and searching. *Nucleic Acids Res.* **2009**, *37*, W202–W208. [CrossRef]
35. Consortium, U. UniProt: A hub for protein information. *Nucleic Acids Res.* **2015**, *43*, D204–D212. [CrossRef] [PubMed]
36. Okonechnikov, K.; Golosova, O.; Fursov, M.; Team, U. Unipro UGENE: A unified bioinformatics toolkit. *Bioinformatics* **2012**, *28*, 1166–1167. [CrossRef] [PubMed]
37. Blum, M.; Chang, H.-Y.; Chuguransky, S.; Grego, T.; Kandasaamy, S.; Mitchell, A.; Nuka, G.; Paysan-Lafosse, T.; Qureshi, M.; Raj, S. The InterPro protein families and domains database: 20 years on. *Nucleic Acids Res.* **2021**, *49*, D344–D354. [CrossRef] [PubMed]
38. Kumar, S.; Tamura, K.; Nei, M. MEGA: Molecular evolutionary genetics analysis software for microcomputers. *Bioinformatics* **1994**, *10*, 189–191. [CrossRef] [PubMed]
39. Wang, Y.; Tang, H.; DeBarry, J.D.; Tan, X.; Li, J.; Wang, X.; Lee, T.-h.; Jin, H.; Marler, B.; Guo, H. MCScanX: A toolkit for detection and evolutionary analysis of gene synteny and collinearity. *Nucleic Acids Res.* **2012**, *40*, e49. [CrossRef] [PubMed]
40. Chen, C.; Chen, H.; He, Y.; Xia, R. TBtools, a toolkit for biologists integrating various biological data handling tools with a user-friendly interface. *BioRxiv* **2018**, 289660. [CrossRef]
41. Bektas, Y.; Eulgem, T. Synthetic plant defense elicitors. *Front. Plant Sci.* **2015**, *5*, 804. [CrossRef] [PubMed]
42. Yan, F.; Li, H.; Zhao, P. Genome-Wide Identification and transcriptional expression of the PAL Gene family in common Walnut (*Juglans regia* L.). *Genes* **2019**, *10*, 46. [CrossRef] [PubMed]
43. Dai, X.; Zhao, P.X. psRNATarget: A plant small RNA target analysis server. *Nucleic Acids Res.* **2011**, *39*, W155–W159. [CrossRef]
44. Shannon, P.; Markiel, A.; Ozier, O.; Baliga, N.S.; Wang, J.T.; Ramage, D.; Amin, N.; Schwikowski, B.; Ideker, T. Cytoscape: A software environment for integrated models of biomolecular interaction networks. *Genome Res.* **2003**, *13*, 2498–2504. [CrossRef]
45. Higo, K.; Ugawa, Y.; Iwamoto, M.; Korenaga, T. Plant cis-acting regulatory DNA elements (PLACE) database: 1999. *Nucleic Acids Res.* **1999**, *27*, 297–300. [CrossRef] [PubMed]
46. Raudvere, U.; Kolberg, L.; Kuzmin, I.; Arak, T.; Adler, P.; Peterson, H.; Vilo, J. g: Profiler: A web server for functional enrichment analysis and conversions of gene lists (2019 update). *Nucleic Acids Res.* **2019**, *47*, W191–W198. [CrossRef] [PubMed]
47. Mering, C.v.; Huynen, M.; Jaeggi, D.; Schmidt, S.; Bork, P.; Snel, B. STRING: A database of predicted functional associations between proteins. *Nucleic Acids Res.* **2003**, *31*, 258–261. [CrossRef]
48. Iquebal, M.A.; Sharma, P.; Jasrotia, R.S.; Jaiswal, S.; Kaur, A.; Saroha, M.; Angadi, U.; Sheoran, S.; Singh, R.; Singh, G. RNAseq analysis reveals drought-responsive molecular pathways with candidate genes and putative molecular markers in root tissue of wheat. *Sci. Rep.* **2019**, *9*, 1–18.
49. Zou, C.; Wang, P.; Xu, Y. Bulked sample analysis in genetics, genomics and crop improvement. *Plant Biotechnol. J.* **2016**, *14*, 1941–1955. [CrossRef]
50. Bolger, A.M.; Lohse, M.; Usadel, B. Trimmomatic: A flexible trimmer for Illumina sequence data. *Bioinformatics* **2014**, *30*, 2114–2120. [CrossRef]
51. Kim, D.; Paggi, J.M.; Park, C.; Bennett, C.; Salzberg, S.L. Graph-based genome alignment and genotyping with HISAT2 and HISAT-genotype. *Nat. Biotechnol.* **2019**, *37*, 907–915. [CrossRef]
52. Pertea, M.; Pertea, G.M.; Antonescu, C.M.; Chang, T.-C.; Mendell, J.T.; Salzberg, S.L. StringTie enables improved reconstruction of a transcriptome from RNA-seq reads. *Nat. Biotechnol.* **2015**, *33*, 290–295. [CrossRef]
53. Tarazona, S.; Furió-Tarı, P.; Ferrer, A.; Conesa, A. *NOISeq: Differential Expression in RNA-Seq—Bioconductor*; Department of Statistics: TU Dortmund, Germany, 2013.
54. Borrill, P.; Ramirez-Gonzalez, R.; Uauy, C. expVIP: A customizable RNA-seq data analysis and visualization platform. *Plant Physiol.* **2016**, *170*, 2172–2186. [CrossRef]
55. Kolde, R.; Kolde, M.R. Package 'pheatmap'. *R Package* **2015**, *1*, 790.
56. Hossain, M.S.; Rasel Ahmed, M.; Ullah, W.; Honi, U.; Tareq, M.Z.; Sarker, M.S.A.; Ahmed, B.; Islam, M.S. Phenylalanine ammonia-lyase gene family (PAL): Genome wide characterization and transcriptional expression in jute (*Corchorus olitorius*). *J. Biosci. Agric. Res.* **2020**, *26*, 2185–2191. [CrossRef]
57. Darzentas, N. Circoletto: Visualizing sequence similarity with Circos. *Bioinformatics* **2010**, *26*, 2620–2621. [CrossRef] [PubMed]
58. Jin, Q.; Yao, Y.; Cai, Y.; Lin, Y. Molecular cloning and sequence analysis of a phenylalanine ammonia-lyase gene from Dendrobium. *PLoS ONE* **2013**, *8*, e62352. [CrossRef] [PubMed]
59. Li, G.; Wang, H.; Cheng, X.; Su, X.; Zhao, Y.; Jiang, T.; Jin, Q.; Lin, Y.; Cai, Y. Comparative genomic analysis of the PAL genes in five Rosaceae species and functional identification of Chinese white pear. *PeerJ* **2019**, *7*, e8064. [CrossRef]
60. Dong, C.-J.; Shang, Q.-M. Genome-wide characterization of phenylalanine ammonia-lyase gene family in watermelon (*Citrullus lanatus*). *Planta* **2013**, *238*, 35–49. [CrossRef]
61. Rushton, P.J.; Reinstadler, A.; Lipka, V.; Lippok, B.; Somssich, I.E. Synthetic plant promoters containing defined regulatory elements provide novel insights into pathogen-and wound-induced signaling. *Plant Cell* **2002**, *14*, 749–762. [CrossRef]
62. Kaur, A.; Pati, P.K.; Pati, A.M.; Nagpal, A.K. In-silico analysis of cis-acting regulatory elements of pathogenesis-related proteins of *Arabidopsis thaliana* and *Oryza sativa*. *PLoS ONE* **2017**, *12*, e0184523. [CrossRef]

63. Yang, H.; Dong, T.; Li, J.; Wang, M. Molecular cloning, expression, and subcellular localization of a PAL gene from *Citrus reticulata* under iron deficiency. *Biol. Plant.* **2016**, *60*, 482–488. [CrossRef]
64. Kong, W.; Ding, L.; Cheng, J.; Wang, B. Identification and expression analysis of genes with pathogen-inducible cis-regulatory elements in the promoter regions in *Oryza sativa*. *Rice* **2018**, *11*, 1–12. [CrossRef]
65. Ren, W.; Wang, Y.; Xu, A.; Zhao, Y. Genome-wide identification and characterization of the Phenylalanine Ammonia-lyase (PAL) gene family in *Medicago truncatula*. *Legume Res. Int. J.* **2019**, *42*, 461–466. [CrossRef]
66. Yuan, W.; Jiang, T.; Du, K.; Chen, H.; Cao, Y.; Xie, J.; Li, M.; Carr, J.P.; Wu, B.; Fan, Z. Maize phenylalanine ammonia-lyases contribute to resistance to Sugarcane mosaic virus infection, most likely through positive regulation of salicylic acid accumulation. *Mol. Plant Pathol.* **2019**, *20*, 1365–1378. [CrossRef] [PubMed]
67. Fukasawa-Akada, T.; Kung, S.-d.; Watson, J.C. Phenylalanine ammonia-lyase gene structure, expression, and evolution in Nicotiana. *Plant Mol. Biol.* **1996**, *30*, 711–722. [CrossRef]
68. Han, H.; Woeste, K.E.; Hu, Y.; Dang, M.; Zhang, T.; Gao, X.-X.; Zhou, H.; Feng, X.; Zhao, G.; Zhao, P. Genetic diversity and population structure of common walnut (*Juglans regia*) in China based on EST-SSRs and the nuclear gene phenylalanine ammonia-lyase (PAL). *Tree Genet. Genomes* **2016**, *12*, 1–12. [CrossRef]
69. Cheng, X.; Wang, S.; Xu, D.; Liu, X.; Li, X.; Xiao, W.; Cao, J.; Jiang, H.; Min, X.; Wang, J. Identification and analysis of the GASR gene family in common wheat (*Triticum aestivum* L.) and characterization of *TaGASR34*, a gene associated with seed dormancy and germination. *Front. Genet.* **2019**, *10*, 980. [CrossRef] [PubMed]
70. Reichert, A.I.; He, X.-Z.; Dixon, R.A. Phenylalanine ammonia-lyase (PAL) from tobacco (*Nicotiana tabacum*): Characterization of the four tobacco PAL genes and active heterotetrameric enzymes. *Biochem. J.* **2009**, *424*, 233–242. [CrossRef]
71. Hamberger, B.; Ellis, M.; Friedmann, M.; de Azevedo Souza, C.; Barbazuk, B.; Douglas, C.J. Genome-wide analyses of phenylpropanoid-related genes in *Populus trichocarpa*, *Arabidopsis thaliana*, and *Oryza sativa*: The Populus lignin toolbox and conservation and diversification of angiosperm gene families. *Botany* **2007**, *85*, 1182–1201.
72. Kaur, H.; Salh, P.; Singh, B. Role of defense enzymes and phenolics in resistance of wheat crop (*Triticum aestivum* L.) towards aphid complex. *J. Plant Interact.* **2017**, *12*, 304–311. [CrossRef]
73. Kumar, A.; Batra, R.; Gahlaut, V.; Gautam, T.; Kumar, S.; Sharma, M.; Tyagi, S.; Singh, K.P.; Balyan, H.S.; Pandey, R. Genome-wide identification and characterization of gene family for RWP-RK transcription factors in wheat (*Triticum aestivum* L.). *PLoS ONE* **2018**, *13*, e0208409. [CrossRef]
74. Chang, A.; Lim, M.-H.; Lee, S.-W.; Robb, E.J.; Nazar, R.N. Tomato phenylalanine ammonia-lyase gene family, highly redundant but strongly underutilized. *J. Biol. Chem.* **2008**, *283*, 33591–33601. [CrossRef]
75. Akdogan, G.; Tufekci, E.D.; Uranbey, S.; Unver, T. miRNA-based drought regulation in wheat. *Funct. Integr. Genom.* **2016**, *16*, 221–233. [CrossRef]
76. Feng, H.; Xu, M.; Gao, Y.; Liang, J.; Guo, F.; Guo, Y.; Huang, L. Vm-milR37 contributes to pathogenicity by regulating glutathione peroxidase gene *VmGP* in Valsa mali. *Mol. Plant Pathol.* **2021**, *22*, 243–254. [CrossRef]
77. Shan, T.; Fu, R.; Xie, Y.; Chen, Q.; Wang, Y.; Li, Z.; Song, X.; Li, P.; Wang, B. Regulatory mechanism of maize (*Zea mays* L.) miR164 in salt stress response. *Russ. J. Genet.* **2020**, *56*, 835–842. [CrossRef]
78. Yamada, T.; Matsuda, F.; Kasai, K.; Fukuoka, S.; Kitamura, K.; Tozawa, Y.; Miyagawa, H.; Wakasa, K. Mutation of a rice gene encoding a phenylalanine biosynthetic enzyme results in accumulation of phenylalanine and tryptophan. *Plant Cell* **2008**, *20*, 1316–1329. [CrossRef]
79. Wu, Y.; Wang, W.; Li, Y.; Dai, X.; Ma, G.; Xing, D.; Zhu, M.; Gao, L.; Xia, T. Six phenylalanine ammonia-lyases from *Camellia sinensis*: Evolution, expression, and kinetics. *Plant Physiol. Biochem.* **2017**, *118*, 413–421. [CrossRef] [PubMed]
80. Wada, K.C.; Mizuuchi, K.; Koshio, A.; Kaneko, K.; Mitsui, T.; Takeno, K. Stress enhances the gene expression and enzyme activity of phenylalanine ammonia-lyase and the endogenous content of salicylic acid to induce flowering in pharbitis. *J. Plant Physiol.* **2014**, *171*, 895–902. [CrossRef] [PubMed]
81. Wang, Z.-B.; Chen, X.; Wang, W.; Cheng, K.-D.; Kong, J.-Q. Transcriptome-wide identification and characterization of *Ornithogalum saundersiae* phenylalanine ammonia lyase gene family. *RSC Adv.* **2014**, *4*, 27159–27175. [CrossRef]
82. Cao, Y.; Meng, D.; Abdullah, M.; Jin, Q.; Lin, Y.; Cai, Y. Genome wide identification, evolutionary, and expression analysis of VQ genes from two Pyrus species. *Genes* **2018**, *9*, 224. [CrossRef] [PubMed]
83. Tufail, M.A.; Touceda-González, M.; Pertot, I.; Ehlers, R.-U. Gluconacetobacter diazotrophicus PAL5 Enhances Plant Robustness Status under the Combination of Moderate Drought and Low Nitrogen Stress in *Zea mays* L. *Microorganisms* **2021**, *9*, 870. [CrossRef]
84. Christopoulos, M.V.; Tsantili, E. Participation of phenylalanine ammonia-lyase (PAL) in increased phenolic compounds in fresh cold stressed walnut (*Juglans regia* L.) kernels. *Postharvest Biol. Technol.* **2015**, *104*, 17–25. [CrossRef]
85. Kervinen, T.; Peltonen, S.; Utriainen, M.; Kangasjärvi, J.; Teeri, T.H.; Karjalainen, R. Cloning and characterization of cDNA clones encoding phenylalanine ammonia-lyase in barley. *Plant Sci.* **1997**, *123*, 143–150. [CrossRef]
86. Joos, H.J.; Hahlbrock, K. Phenylalanine ammonia-lyase in potato (*Solanum tuberosum* L.) Genomic complexity, structural comparison of two selected genes and modes of expression. *Eur. J. Biochem.* **1992**, *204*, 621–629. [CrossRef] [PubMed]
87. Xu, F.; Deng, G.; Cheng, S.; Zhang, W.; Huang, X.; Li, L.; Cheng, H.; Rong, X.; Li, J. Molecular cloning, characterization and expression of the phenylalanine ammonia-lyase gene from *Juglans regia*. *Molecules* **2012**, *17*, 7810–7823. [CrossRef] [PubMed]

88. Dixon, R.A.; Maxwell, C.A.; Ni, W.; Oommen, A.; Paiva, N.L. Genetic manipulation of lignin and phenylpropanoid compounds involved in interactions with microorganisms. In *Genetic Engineering of Plant Secondary Metabolism*; Springer: Berlin/Heidelberg, Germany, 1994; pp. 153–178.
89. Pearce, S.; Vazquez-Gross, H.; Herin, S.Y.; Hane, D.; Wang, Y.; Gu, Y.Q.; Dubcovsky, J. WheatExp: An RNA-seq expression database for polyploid wheat. *BMC Plant Biol.* **2015**, *15*, 299. [CrossRef] [PubMed]
90. Ma, J.; Ding, P.; Qin, P.; Liu, Y.-X.; Xie, Q.; Chen, G.; Li, W.; Jiang, Q.; Chen, G.; Lan, X.-J. Structure and expression of the *TaGW7* in bread wheat (*Triticum aestivum* L.). *Plant Growth Regul.* **2017**, *82*, 281. [CrossRef]